Increasing Efficiency of Hybrid Electric Vehicles Using Advanced Controls

by

Patrick Ellsworth

A thesis

presented to the University of Waterloo

in fulfillment of the

thesis requirement for the degree of

Master of Applied Science

in

Mechanical and Mechatronic Engineering

Waterloo, Ontario, Canada, 2016

AUTHOR'S DECLARATION

This thesis consists of material all of which I authored or co-authored: See Statement of Contributions included in this thesis. This is a true copy of the thesis, including any required final revisions, as accepted by my examiners.

I understand that my thesis may be made electronically available to the public.

Abstract

The drive to improve and optimize hybrid vehicle performance is increasing with the growing market of hybrids. This research is conducted on a student developed parallel split hybrid architecture. The architecture features an engine, transmission and two electric motors; one pre-transmission and one post-transmission. In order to complete this project, UWAFT has selected an 850 cc two-cylinder turbocharged engine that will operate on 85 % ethanol (E85) in a plug-in hybrid parallel split powertrain configuration. As most production hybrids have four-cylinder engines, this powertrain is seen as further electrification of hybrid electric vehicles. Different tests are conducted to demonstrate how the engine would operate in the vehicle. The results show that by running E85, the engine is able to produce up to 58% of the specified power rating with its first tune and provided validation for the capability of producing power in parallel operation. Additionally the model more accurately represents the speed matching capabilities of the engine.

The control strategy operates the powertrain components in a series, parallel, and all electric power flow. Control strategies for these three power flows are compared through optimization of efficiencies within the powertrain. The resulting control strategy optimizations used by the team have increased the vehicle's charge depleting range by 27.7 %., while decreasing energy consumption by 13.8 %.Additionally it produced a 30.5 % increase in miles per gallon gasoline equivalent in charge sustaining mode, increasing total range by 30.2%.Inspection of cell internal resistance (R_{int}) derived by the hybrid pulse power characterization (HPPC) tests indicates that R_{int} is a function of relative capacity (state of charge, or SOC), thus some SOC ranges are more efficient than others. Therefore energy losses can be minimized by placing charge sustaining operation in a more efficient SOC range. This creates three operational stages; the initial charge depleting stage to an efficient SOC, a charge sustaining stage until a recharge station is within reach, and a final charge depleting stage until arrival. When coupled with a known drive distance, this three segment Internal Resistance Based (IRB) control strategy increases the extended range electric vehicle (EREV) net battery efficiency from 96.8 to 97.3 % with an associated 14 % decrease in energy losses across the urban domestic drive schedule. Indirect benefits include an increased active SOC range, decreased urban emissions, and decreased waste heat generation, meeting the goals of Advanced Vehicle Technology Competitions.

Acknowledgements

I would like to thank my family for always supporting me through my continued education; my team members for allowing me to complete my research in the best and most unique way; and Dr. Fraser and Dr. Fowler for making it all possible.

Table of Contents

List of Figures

List of Tables

List of Acronyms

AVTC	Advanced Vehicle Technology Competition
BEV	Battery Electric Vehicle
BMS	Battery Management System
CAFE	Corporate Average Fuel Economy
CAN	Control Area Network
CO_2	Carbon Dioxide
DOD	Depth of Discharge
DFMEA	Design Fault Mode Effect Analysis
E&EC	Emissions and Energy Consumption
EMI	Electromagnetic Interference
EREV	Extended Range Electric Vehicle
FEA	Finite Element Analysis
FDR	Final Design Report
FTA	Fault Tree Analysis
HV	High Voltage
HWFET	Highway Fuel Economy Driving Schedule
ICE	Internal Combustion Engine
IRB	Internal Resistance Based
LV	Low Voltage
MIL	Model In the Loop
OBD	On-Board Diagnostics
PHEV	Plug-in Hybrid Electric Vehicle
SOC	State of Charge
UDDS	Urban Dynamometer Drive Schedule
UWAFT	University of Waterloo Alternative Fuels Team
VPC	Vehicle Propulsion Controller
VTS	Vehicle Technical Specifications

Chapter 1
Introduction

The automotive market is making the push for vehicles that are more efficient and have more thrilling technology. Given the current consumer transportation market, gasoline vehicles are the most popular option, securing the majority of vehicle sales [1]. However, as the availability and cost of electric, automotive-grade drivetrain components increase, this topology is shifting. Modern consumers are both comforted by the purchase of a reduced-emissions vehicles and interested in the performance advantages offered by electric propulsion. Extended range electric vehicles (EREV), just one of many hybrid architectures, are a rapidly growing market, experiencing an increase of more than 80 % additional sales when compared to recent years (2012 - 2013) [2].In addition to the market demand Vehicle electrification is a key initiative by automakers to improve fleet fuel efficiencies in accordance to planned Corporate Average Fuel Economy (CAFE) standards [3]. The incorporation of an electric powertrain in conjunction with a conventional internal combustion powertrain helps to increase overall vehicle energy efficiency and reduce emissions [4][5][6]. As a result, Hybrid Electric Vehicles (HEVs) and Plug-in Hybrid Electric Vehicles (PHEVs) have seen a substantial increase in market share as seen in Figure 1.[7]

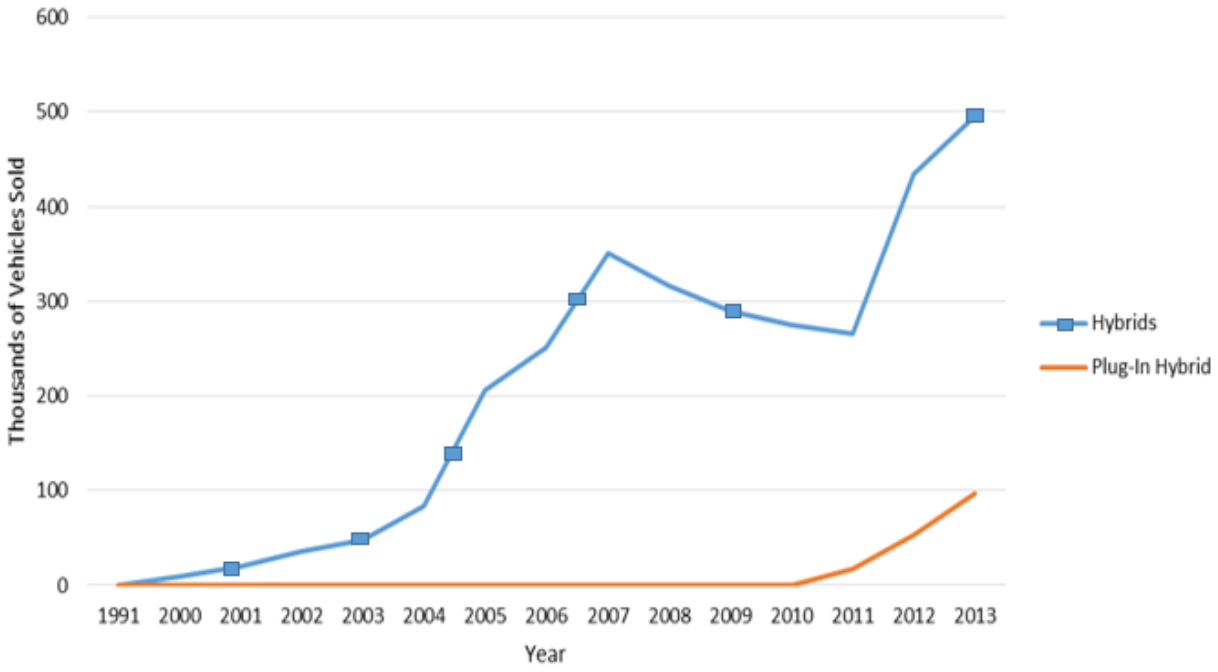

Figure 1:Hybrid and Plug-in Hybrid Vehicle Sales

The objective of this report is to highlight the significant efficiency increases that can be achieved with advanced technics, components, and controls of hybrid powertrains. A hybrid vehicle can offer significant advantages over the conventionally powered competition regarding performance and fuel economy through the utilization of a blended powertrain[4]. With the Chevrolet Bolt and the Tesla Model 3 becoming production ready in the next two years, new reasons for purchasing hybrids will need to be explored as it will no longer be the most environmentally affordable option on the market. This is driving a demand for vehicle improvement at all levels of the vehicle, from the fuel we use to the vehicle level controls. This report will address various strategies for advanced efficiency changes.

The aforementioned push to advanced electrification of vehicles has incentivized General Motors and the United States Department of Energy to partner together and create a competition to drive research and education in the hybrid industry. This advanced vehicle technology competition has been through much iteration the most current is EcoCAR 3. EcoCAR 3 is a four-year engineering collegiate competition that challenges 16 teams from universities across North America to re-engineer a 2016 Chevrolet Camaro while maintaining the vehicle's muscle car appearance. The

vehicle is expected to be eco-friendlier with its reduced greenhouse gas emissions due to the usage of alternative fuels. Additionally, consumer acceptability and safety are priorities while simultaneously increasing the vehicle performance and using cutting-edge automotive technology. The competition is sponsored by General Motors and the U.S. Department of Energy, and managed by Argonne National Laboratory[8]. It is through the competition provided vehicle research platform, software programs, and industrial sponsorship that the research in this paper was developed.

The team at the University of Waterloo that competes in the competition is the University of Waterloo Alternative Fuels Team (UWAFT). UWAFT's selected design is a parallel series split plug-in hybrid electric 2016 Camaro. This powertrain, outlined in Figure 2, makes advanced steps in vehicle electrification, increasing electric power while reducing the size of the conventional combustion engine. This powertrain includes a Textron 850cc turbocharged Multi-Purpose Engine (MPE850), two GKN AF130-4 electric motors, a General Motors 8L45 automatic transmission, a General Motors electronically limited slip differential (eLSD), and A123 16.2 kWh battery.

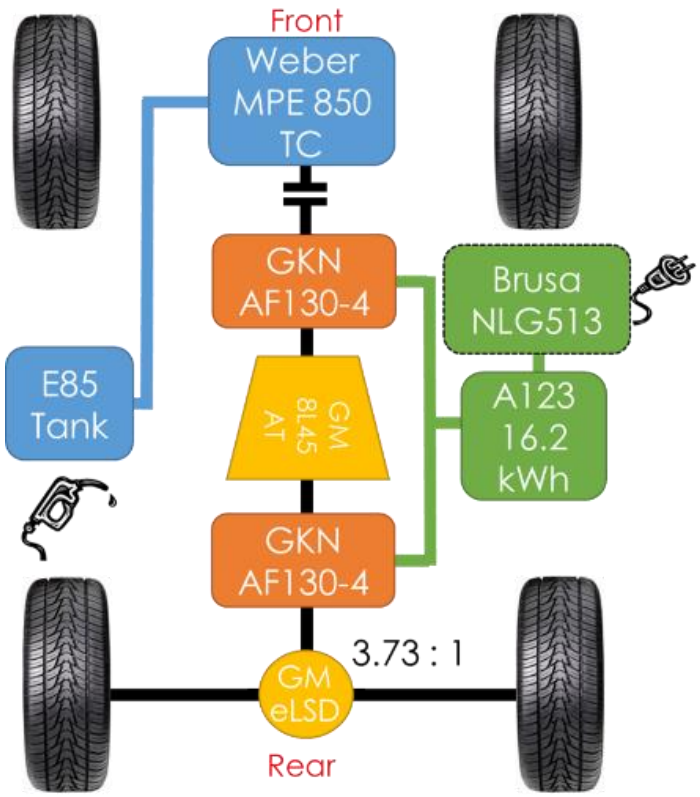

Figure 2: Diagram of UWAFT parallel series split plug-in hybrid electric powertrain

This powertrain allows for three modes of operation: series, parallel, and all-electric. The first two operation modes utilize the engine but in different capacities. The engine is not required for the all-electric operation. In series operation, the 8L45 transmission is in neutral, thus decoupling all the pre-transmission components from the road. The result is that only the post-transmission motor can power the road. However, the engine and pre-transmission motor can act as a generator to supply electricity to the powertrain. The series operation would occur solely when the A123 battery does not have sufficient capacity and is thus a charge-sustaining operation.

The parallel operation mode, will occur in both charge sustaining and charge depletion operations. In this operation, all components can provide power to the road through the rear differential. When the A123 battery is depleted, the MPE850 engine will provide the majority of the power with the electric motors supplementing the power during acceleration. When the A123 battery still has sufficient charge the engine will only be used to maximize power when the driver requests more power than what the motors are capable of providing.

During these two operational modes, the engine will operate differently. The tests that are examined in the third chapter are to validate that the MPE 850 engine can operate in all of the required modes. Individual tests that are specific to the operational modesare conducted, and the performance is examined to validate its use in the larger system. These tests include performance parameterization but also the ability of the engine to switch between different modes. In addition to the operation modes the third chapter will address modifying the engine from gasoline to ethanol. This change allows the vehicle to reap the benefits of the fuels extremely green well to pump emissions, as well as the benefits of the high efficiency turbo engine at the pump to wheel. A custom set up for dynamometer and controller is required for the engine to operate on ethanol fuel. The paper will elaborate on how this is done and how this change effects the performance and energy efficiency of the engine.

Though PHEV sales are increasing, there are aspects of their design which are limiting their economic growth; specifically vehicle electric range and battery capacity which causes "range anxiety"[9]. Increasing the electric driving potential of the vehicle can increase the payback for the consumer, thereby making PHEVs more marketable.Developing optimized control strategies increases the vehicle electric range and the per kilometer monetary savings, without any increase in component cost. The fourth chapter outlines the team's modeling, simulation and control development in the first year of the competition as part of the process of re-engineering the Chevrolet Camaro. It will outline the modeling techniques that the team has implemented and outline the path forward for the following three years of the competition. Specifics on component models, limitations and efficiencies developed by UWAFT will be presented. Control strategies will be discussed and compared for all three modes of the vehicle's operation alongside overall vehicle-level results.

While extensive research [10] has been performed regarding batteries and battery models, comparatively few improvements have been made in battery management and vehicle propulsion control systems (BMS, VPC).Since battery voltage, internal resistance, and degradation rate are not asymmetrically constant, an ideal operating capacity exists.The objective of the work in the fifth chapter is to seek an implementation strategy for Just-in-Time control. An Internal Resistance Based (IRB) Just-in-Time control strategy is proposed that reduces the power loss by operating within an ideal capacity range. The ideal SOC range is determined by parameterizing

the Rint model through hybrid pulse power characterization (HPPC) tests. The benefits of the IRB control scheme are then estimated by vehicle powertrain modeling.

Chapter 2
Background

E85 is a type of ethanol fuel which is composed of 85% of denatured ethanol fuel and 15% gasoline. Three advantages of using E85 over the conventional gasoline are the reduction in exhaust emissions[11], the reduction of dependence on gasoline through diversification of fuel sources, and the utilization of waste materials to produce ethanol in certain areas [12]. These benefits have led to UWAFT's selection of ethanol, 85% grade, for the EcoCAR 3 competition.

In pursuit of minimizing the environmental impact of UWAFT's ethanol-fueled, hybrid Camaro; a downsized and turbocharged engine is selected in place of the stock, gasoline, V6 engine. This approach of downsizing and turbocharging is an industry-recognized pathway to reducing fuel consumption [13]. This reduced fuel consumption alongside the utilization of E85 fuel have a reduced impact on well-to-tank emissions in comparison to standard gasoline vehicles [14].

In hybrid vehicles, powertrain component testing such as dynamometer testing serves to refine further the hybrid supervisory controller (HSC) operation mode selection algorithm and to optimize overall vehicle efficiency. In HEV's with charge-sustaining operation modes, the engine-generator coupling means that the optimal internal combustion engine's (ICE) operating torque and speed is not necessarily aligned with the generator's optimal efficiency point. Existing HEVs with appropriately tuned operation modes provide an increased vehicle efficiency with short-term, high-power charge-sustaining operation, despite non-optimal engine performance [15]. In pursuit optimal vehicle efficiency UWAFT needs to gather dynamometer results over a range of operation points.

Electric vehicles are evolving to incorporate multiple gear gearboxes in an effort to increase energy efficiency and performance of electric powertrains. It has been demonstrated that implementing a two speed gearbox can achieve a 7.31 % fuel economy improvement in the UDDS drive cycle alone[16]. Increasing the number of gears has shown to improve both energy efficiency and performance of EVs, which suggests the possibility that high efficiency transmissions may potentially increase electric powertrain efficiency, resulting in larger electric range.

The type of gearbox has been examined in multiple works[9][16][17]. Previous work has been completed by Wager et al examining the difference between utilizing automatic and manual transmissions in an electric vehicle. The work demonstrated that a manual transmission consumed less energy than an automatic transmission, thereby increasing the Electric Vehicle's (EV) electric range. It is noted in the work, however, that the control of the automatic transmission was not complete and therefore that the resulting gear selection was not optimal. The work also utilized a single gear for each transmission test, not allowing for optimal gear selection. It is hypothesized then, that integrating multiple gears and utilizing the optimal control of an automatic transmission would therefore greatly increase energy efficiency and the electric range of the electric powertrain[17].

It has been shown that battery performance is a function of relative capacity (state of charge, or SOC) (Figure 3)[18][19][20]. Modern vehicle controllers do not take advantage of this asymmetrical performance, and frequently operate outside of the ideal capacity range [21][22]. It is desirable to develop a control strategy that operates within the ideal range for as long as possible.

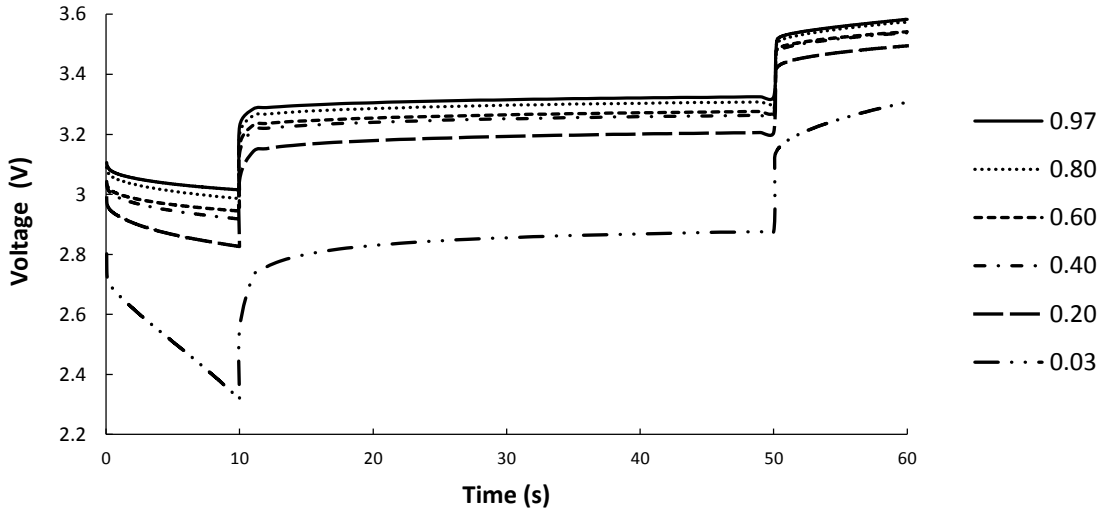

Figure 3: Commercial $LiFePO_4$ battery HPPC voltage response at different SOCs [this work]

Control methods for EREVs are typically allocated into two distinct modes, charge depleting (CD) and charge sustaining (CS) [23]. During charge depleting mode the battery is the primary

energy source for the vehicle. Once the battery has been depleted to a minimum capacity, the EREV begins charge sustaining mode which utilizes the engine to recharge the battery 1~2 % above the minimum capacity before the battery resumes discharge. Traditionally, the minimum capacity for EREVs is 19 % SOC[21], resulting in a gradual capacity decline (Figure 4). The 19 % threshold is a compromise between minimizing battery degradation that occurs at lower SOCs, and maximizing battery energy storage [22][24].

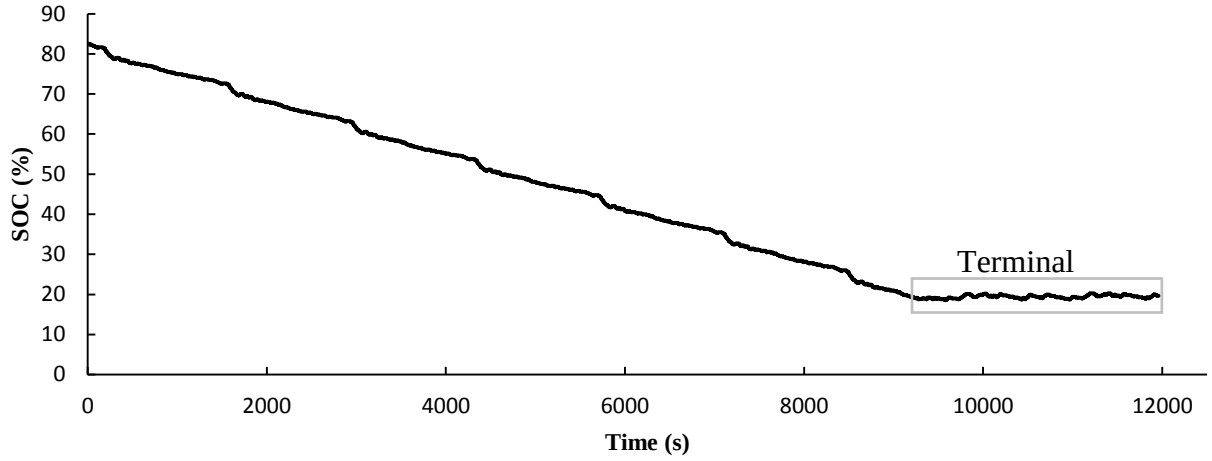

Figure 4: EREV using traditional controller over the urban domestic drive schedule (UDDS)

An alternative, "Just-in-Time," control strategy has been proposed [25] that allows the CS mode to operate within more favorable SOC ranges, assuming the vehicle can deplete its battery immediately prior, or 'just in time,' to reaching a recharge station. A visual representation of Just-in-Time control, which utilizes an additional CD mode to exhaust the battery, is shown in Figure 5.

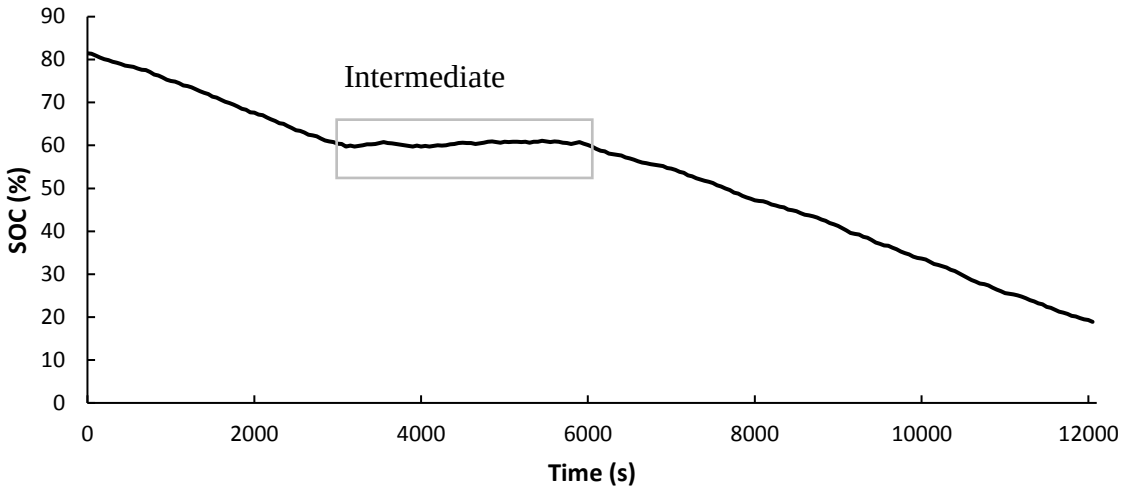

Figure 5: EREV using Just-In-Time controller over the urban domestic drive schedule (UDDS)

Chapter 3

Validation of a Two-Cylinder Engine in a Plug-in Hybrid Electric Camaro for EcoCAR 3

3.1 Goals and Scope of Work

The main goal of this work is to compare the effectiveness of two control strategies: parallel operation and series operation during charge sustaining. These control strategies are developed through a case study examining a constant speed highway cruising operation. Though this case study will help the team validate its control strategy, it also allows the team to validate data through the bench testing of the MPE850 engine with both E10 and E85. The data collected validates the teams design decision to go with a smaller two-cylinder engine and reduce emissions while maintaining performance. The main goal will, therefore,be reached by meeting the following objectives in sequence:

1. The ability to achieve basic engine functionality and control
2. Validate data from previous works on engine performance
3. Validate design decisions by demonstrating how the engine operates in the larger system
4. Collect data to further refine the engine model
5. Compare series and parallel control operations with real engine data

The subsequent sections detail how the engine was tested to validate its use in the vehicle powertrain. After a brief background on engines in hybrid vehicles, the methodology section details what tests are conducted and how, and the results and analysis discuss the validation of the design by examining the results of the tests. The author's findings are then summarized in the conclusions.

3.2 Methodology

To utilize the selected ethanol fuel and downsized engine effectively, UWAFT needs to develop an engine tune for the Weber MPE 850 engine which enables it to operate effectively given throttle demands. This tuning is defined in the form of an engine base map, and it is developed with the use of a dynamometer testing apparatus [26]. The engine dynamometer UWAFT has

access to maintain a set engine speed while monitoring the developed torque, speed and stoichiometric efficiency amongst other engine parameters. The result of a well-developed base engine map is an optimal, reliable engine output over a range of throttle demands [26].

A test benchdesign is created to collect data and validate the engine model, thus meeting all objectives and the goal of this work. This bench set up includes the MPE850 engine but also systems to control and obtain information. A MoTeC controller controls the engine while the controller and a DYNOmite water brake dynamometer gather information. This setup can be seen in the following two figures and further explained in the subsequent sections.

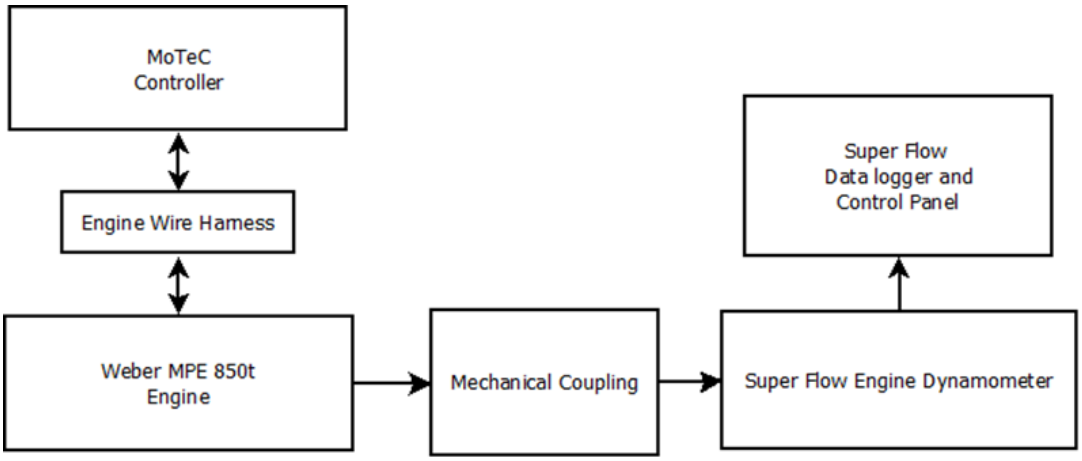

Figure 6: Diagram of test bench setup for MPE850 engine

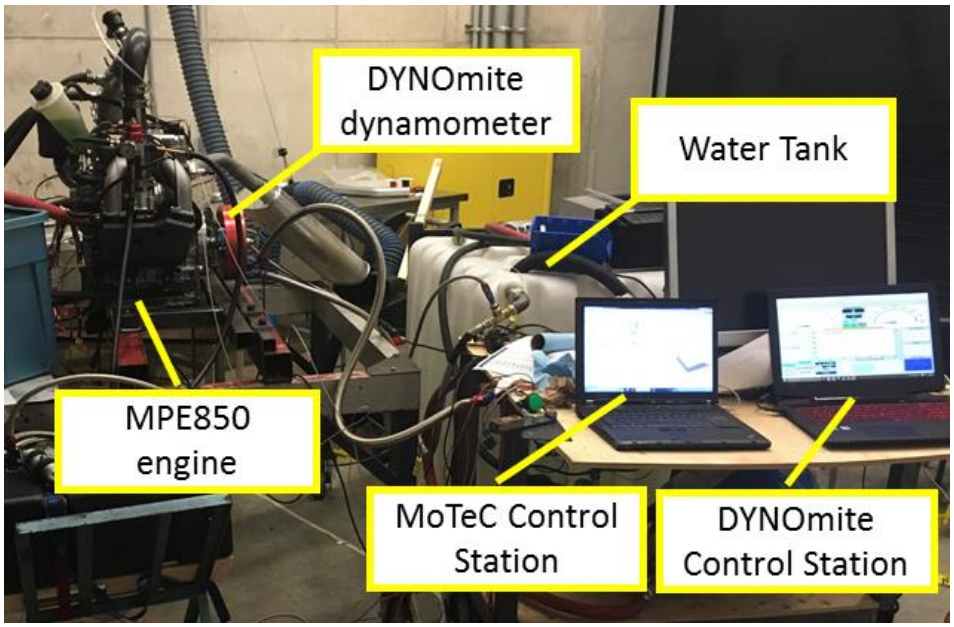

Figure 7: Picture of test benchsetup with callout of important components

3.3 MPE850 Engine

During previous feasibility studies and a powertrain proposal for the competition,an MPE 850 cc turbocharged engine was selected from Wasteland Performance. The engine is not an automotive engine however it is EPA certified for off-road use, including snowmobile and marine applications.

One of the reasons the engine was selected was due to its mass as previously mentioned. The engine is only 59 kg which is 98 kg lighter than the stock LFX V6 engine[27]. This mass reduction is important because of the increased vehicle mass due to the addition of two electric motors and a battery pack. The Weber engine will also free up more space in the engine bay for the addition of new components such as the P2 inverter and the high voltage distribution box etc.Though it is a significantly smaller engine the power to weight ratio of the engine is slightly higher at 1.56 kW/kg versus 1.54 kW/kg[27][28]. All specifications for the engine can be found in Table 1.

Table 1: MPE 850 performance characteristics[28]

Performance Metric	Value	Unit
Engine Class	Multi-Purpose Engine, Inline, 2-cylinder	N/A
Cylinder Volume	850	cc
Peak Power	92	kW

Peak Torque	120	Nm
Max Speed	8000	rpm
Max Speed in System	5000	rpm
Mass	59	kg

To operate the engine three systems were added. The first system is an intercooler. The intercooler selected is an air-liquid intercooler to maximize performance in the limited space in the engine compartment. The second system that was added is a fuel delivery system. The system is capable of delivering 298 L per hour at a pressure of 4 bar. Finally, the oil system needed to be installed. As it is a dry sump the oil must be raised to the same level as the engine. The final set-up can be seen in Figure 8.

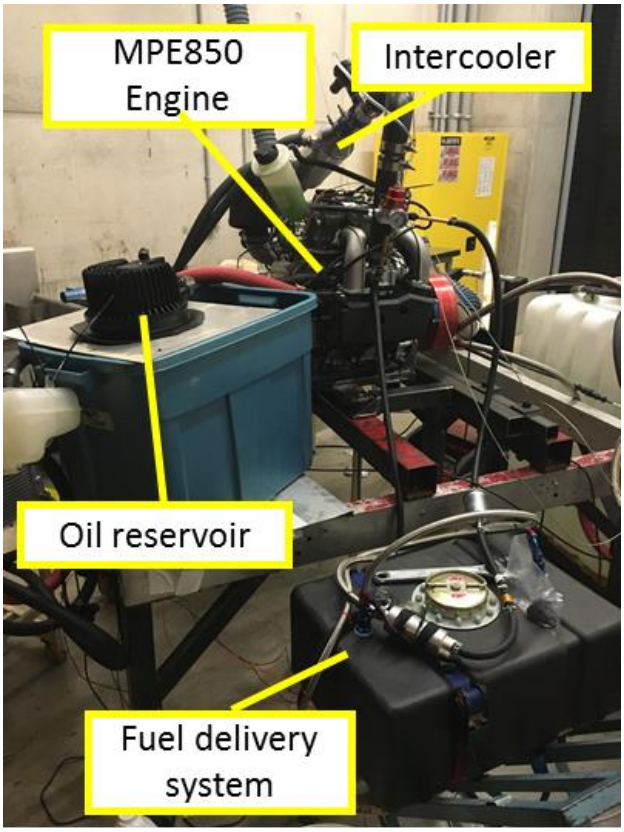

Figure 8: Picture of engine set up with callout for important additions for engine operation

3.3.1 Engine Dynamometer

A water break engine dynamometer is utilized to measure the power and torque delivered by the engine.As the engine is often used in snowmobile applications, a 9” single rotor DYNOmite snowmobile dynamometer is used on the test bench. The dynamometer is capable of measuring more torque than the engine can supply, 386 Nm, and reach speeds greater than 14,000 rpm. The testing capabilities of the dynamometer are more than sufficient to measure power and torque for the MPE 850 engine. The dynamometer is connected to the tapered shaft of the engine, so it is a direct measurement of the engine.

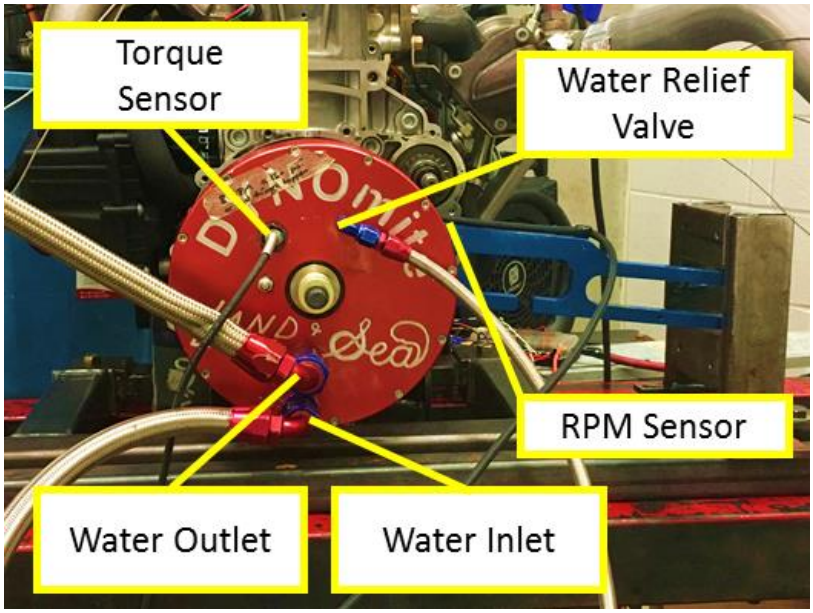

Figure 9: DYNOmite engine dynamometer with callouts for important components

3.3.2 MoTeC Engine Controller

Though the engine came with a controller, an M400MoTeC controller was selected to be the Engine Control Unit (ECU). The controller was selected due to the familiarity of the unit and level of control through a user-friendly interface that the ECU offers. It is also able to read all important information required by the team, including fuel consumption for fuel economy calculations.

Some more advanced features were purchased as add-ons for the ECU to enable proper engine control. The ECU was purchased with drive by wire, advanced functions, wide lambda sensing,

and data logging. These functions are important for control of the engine. Most notably, the drive by wire capability as the engine will not be controlled by the pedal but rather a supervisory controller. A wide band lambda sensor is necessary to enable better tuning due to the E85 conversion.

3.3.3 System Modeling Details

UWAFT's modeling was originally developed in Autonomie, vehicle-modeling software developed by Argonne National Laboratory. Autonomie is a software wrapper which runs on top of MATLAB/Simulink, and auto-generates models to run in the Simulink environment. UWAFT began its modeling process by using default vehicles and models within Autonomie, relying on component models for items such as engines and motors which are independently validated by the suppliers. UWAFT also generated its own models for new components proposed for vehicle integration, and began running the vehicle simulations within the Simulink environment once the initial modeling stage was completed. The UWAFT vehicle architecture power flow from Autonomie can be seen below inFigure 10.

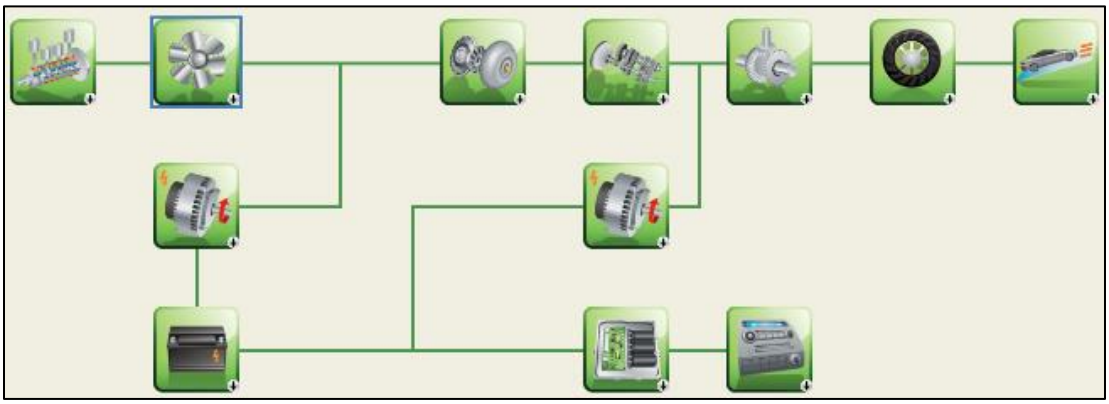

Figure 10: Split-parallel PHEV Powertrain Diagram in Autonomie

The models developed by Autonomie and UWAFT both use look-up tables as the backbone of the development. Look up tables are ideal for the teams use, allowing quick simulations and easy development using empirical data sets. Table 2 is a summary table of all components in the vehicle model.

Table 2: Powertrain Components

Component	Manufacturer/Model	Specifications
Engine	Weber MPE 850cc Turbo	PP: 92 kW

P2/3 Motor	GKN AF130-4	PP: 70 kW (300 V)
		PP: 70 kW (300 V)
Battery	A123 6x15s3p	Cap: 16.2 kWh
		N Volt: 292 V
Transmission	GM AT	8 Gear, Longitudinal Auto
Final Drive	GM 3.73 Final Drive, eLSD	3.73 : 1 Final Drive Ratio

Note: PP: Peak Power, PC: Peak Current, CP: Continuous Power, Cap: Capacity, N: Nominal, eLSD: Electronic Limited-slip differential

The multiple power flow operations of the powertrain require multiple equations that model the engine and the power requirements. In the series operation where energy efficiency of the engine and the P2 motor is maximized, the control is such that the engine's efficiency matches the motor's peak efficiency; maximizing generation efficiency of the engine while employing a thermostatic control strategy. During parallel operation, it is required that the motors and engine be capable of providing the peak wheel torque and maximizing the acceleration of the vehicle. The MPE850 manages to provide an efficient power that lines up with the GKN motor peak efficiency while also producing sufficient power to work in parallel with the motors for vehicle propulsion.

3.3.4 Engine Map Data

In developing an ethanol performance map for the Weber MPE850, UWAFT will perform a series of dynamometer tests. Currently, UWAFT has a gasoline torque versus speed map for the Weber MPE 850, shown in Figure 25. The results of this paper will be used to generate an ethanol map.

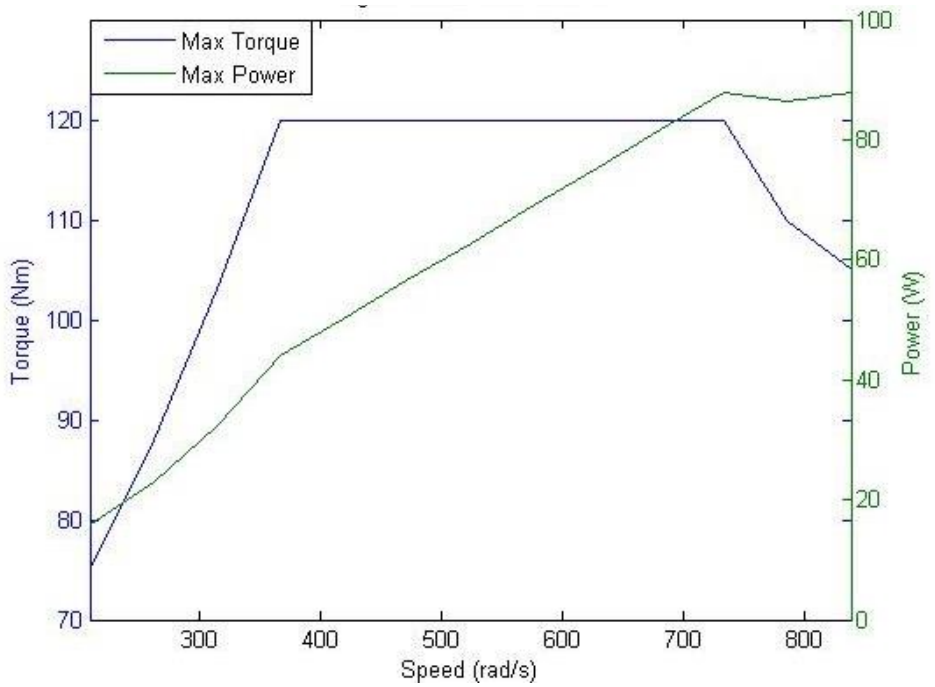

Figure 11: Weber Performance Curve

3.3.5 Engine Startup SOFT ECU

To simulate the engine startup within the vehicle system models, a SoftECU is developed to create the pathways by which the engine could enter into a start-up, shut-down, or emergency shut-down procedures (in the case a fault is encountered). The role of SoftECUs, in a software model, are to simulate physical Electric Control Units (ECUs), replicating the functionality of real ECUs at the vehicle system level. The SoftECU communicates with the HSC using CAN messaging to translate current operational parameters of the engine and other components to the SoftECU to determine if the engine can start-up or if it should shut-down. The transitions thought the stages of operation of the SoftECU are depicted in Figure 12.

As the vehicle being developed is a hybrid electric vehicle, and the vehicle architecture allows the car to operate in different modes of operation (full EV, series, and parallel) the engine does not have to be on the entire time the vehicle is running. Once the Lithium Ion Battery reaches a particular threshold SOC (25%) the engine must turn on to enter into one of the operating states. The request to have the engine "turn on" is read by the HSC and transmitted to the SoftECU. This contorl sequence is just the first step, though, before start-up can be achieved more information must be acquired.

Besides the SOC of the battery and the request from the HSC to operate, the engine also requires data on its current state. Readings of temperature, pressure, and operating signal from SoftECU are sent to the HSC from the SoftECU to determine the "health" of the engine. Detection of errors and faults result in degradation of the "health" of the component and must be mitigated before start-up can be achieved. If no faults exist, the engine is considered as "healthy" by the HSC and signals the SoftECU to begin start-up procedures, moving the engine component state from the Engine STOP position (Stage 0) to the Engine START state (Stage 1). Theses controls are necessary from a safety aspect and are critical for accurate simulation results.

In the Engine START state, the starter initiates engine operation, but before torque is transferred to the other driveline components the engine must be coupled to the driveline through the clutch. The clutch requires that the motor and engine be the same speed before this can take place (Stage 1.5). Otherwise, the clutch system would be damaged. Clutch engagement is then allowed to take place, coupling engine to driveline, and the SoftECU runs system checks to ensure the stability of operation (Stage 2).

Once the clutch has safelytransitioned, and the conditions for safe operation of the system are met, the HSC operating mode is capable of transitioning to a series or parallel operation mode. Determination of the vehicle state being either "series" or "parallel" is determined based on the Vehicle State Machine controls logic from the HSC.Should a fault occur during operation the system enters into emergency shutdown procedures and the system moves to the Engine STOP state (Stage 0). Any faults encountered are then mitigated by the system’s HSC.

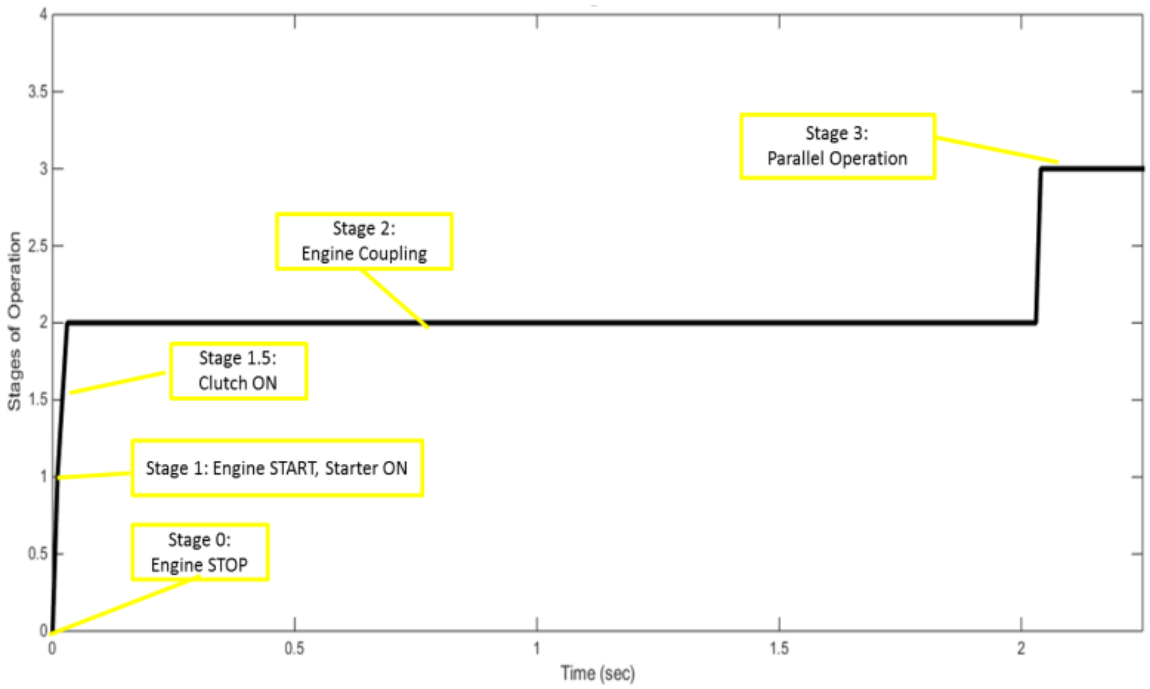

Figure 12: Stages of Transition in Engine SoftECU

The SoftECU transmits data of engine operation and overall health to the HSC. Constant updates ensure that torque application can be achieved and the components will not be damaged. The SoftECU also accounts for transitions between Series and Parallel, being able to transition between operations if required.

3.3.6 Limitations of Extrapolations

The model does use almost exclusively look up tables, with linear interpolation. These have an inherent inaccuracy between measured values in the map, relying on a linear approximation between the points.

Additionally the entire vehicle model consists of varying fidelity models. They do not take into effect thermal interactions between each other and do not handle transient operation accurately. These two areas of error become significant when looking at vehicle control. The experiment is design to minimize the effect of these errors as much as possible.

3.4 Controller Network Overview

The engine and its etcetera necessary peripherals are modulated through both the HSC and the dedicated engine controller shown in Figure 13.

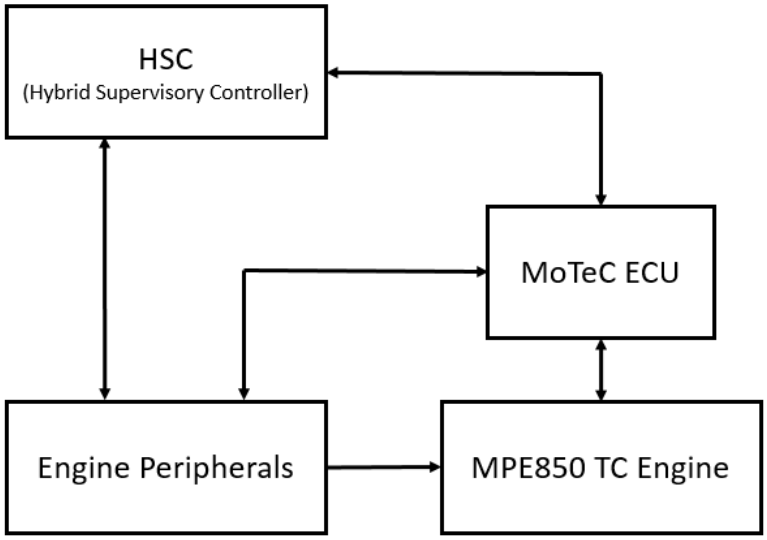

Figure 13: Controller Network Overview Diagram

The diagram previous displays the hierarchy of thecontroller network of the engine in the system of a car. The HSC controls the engine operations at a system level, the MoTeC ECU regulates most actions at a component level, and the engine plant and peripherals respond to the commands of the controllers to actuate the engine.

The HSC's main role in controlling the engine is to achieving system level control strategies, such as using different engine start procedures to engage directly to performance mode, or enter change sustaining mode. Its input and output signals are mostly digital signals to the engine peripherals to engage relays, indifferent configurations and IO pins on the MoTeC ECU to change the state that the ECU operates at. An important HSC output signal is the driver throttle request to the MoTeC which is used to specify the demand to the engine. This signal is typically an analog voltage signal in a normal automotive application, but in the case of this application, this signals will be sent over a CAN network.

The MoTeC ECU regulates values that are more important at a component level. The MoTeC ECU will receive commands from the HSC to determine its operation mode and ensure safe component operation. The ECU mainly interacts with the engine peripherals and sensors, such as injectors, ignition coils, lambda sensors and the throttle body to ensure normal component functionality, while also handling peripheral PID controls such as in DWB functions.

3.5 Control Strategy Verification

The verification of the engine control strategy focuses on the interaction between the MoTeC ECU, the engine peripheral and plant. The ECU control strategy shall be closely analyzed as it is the controller that greatly affects the efficiency and power output of the engine. The current controller network is designed so that the HSC outputs a few digital signals and the throttle request, the test bench uses a physical throttle and switches to send the appropriate signals needed to test the ECU. The main signals used by the ECU to control the engine are listed in tables below.

Table 3: MoTeC ECU Main Inputs

Signal Name	Signal Units	Use
starter_on	Digital	Signals the ECU to power and actuate the starter relay
igniton_pwr	Digital	Signals the ECU to provide power or kill the ignition
throttle_request	Percent	Delivers the requested throttle body position
fuel_pump_pwr	Digital	Signals the ECU to power and actuate the fuel pump relay

Table 4: MoTeC ECU Main Outputs

Signal Name	Signal Units	Use
inj_ctrl	Digital	Injector open command
tb_motor	Percent	The throttle body position command
ign_ctrl	Digital	Ignition spark command

Table 5: Engine Peripheral Main Outputs

Signal Name	Signal Units	Use
cam_eng_spd	RPM	Engine speed detected by the cam sensor
tb_pos	Percent	The throttle body position detected by the position sensor
lambda	Ratio	The exhaust lambda value
eng_temp	°C	The temperature of the engine
manifold_air_pres	kPa	The pressure in the intake manifold

The input signals in Table 3 are used by the ECU to determine the commanded operation of the engine which can be transmitted by the HSC in the vehicle. The main outputs in Table 4 are used to regulate the actions of the engine, and the peripheral feedbacks in Table 5 are used again to alter the output

To acquire data on the performance of the engine and validate the control strategy, the dynamometer adjusts the negative torque that is applied to the engine while recording the engine RPM and torque. The ECU output is altered based on the context of creating the different vehicle operation modes and the dynamometer can be used to determine the points.

3.5.1 Series Operation

In the series operation, the engine's primary goal is to operate at a constant speed and torque output to create the most energy efficient generation set. The engine speed will be limited to specific test points by the dynamometer, and the torque output and fuel consumption will be measured to determine the efficiency of the engine as shown in Figure 14. This testing methods verifies the performance of the engine in a situation where the torque of the P2 motor can be adjusted to create the most efficient generation set.

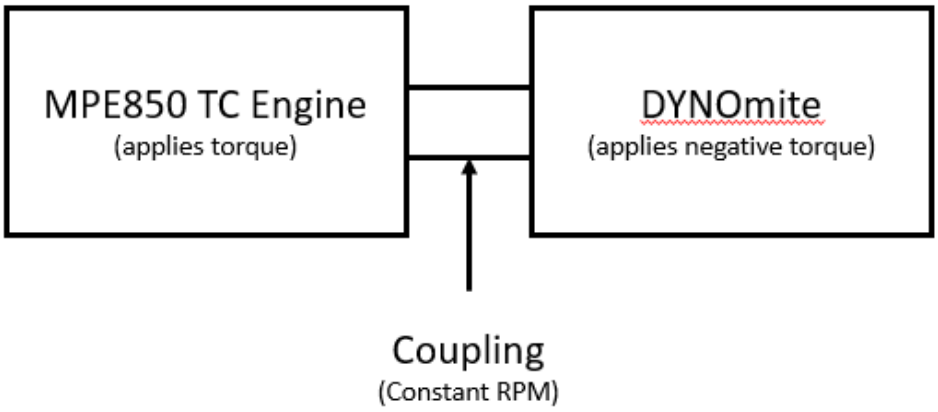

Figure 14: Block diagram showing coupling between engine and dynamometer

By altering the throttle command to MoTeC ECU, the throttle body position is changed, commanding the engine to produce more torque. The control strategy being verified will attempt to create a varying torque levels while the speed is maintained by an opposite torque of the dynamometer. By collecting data about the steady state operation of the engine with this control

strategy, the controller can be set to run in a mode to produce constant torque and speed to maximize generation efficiency.

3.5.2 Parallel Operation

In parallel operation at a constant speed, the speed of the engine must match a specific required speed which is determined by the vehicle speed and transmission gear ratio. The torque produced by the engine can be adjusted to operate at a most efficient point of the powertrain. This method can be verified with the same testing method to verify the series operation, but the set point of engine speed is no longer determined by the generation efficiency, and the aim of the controller is to operate the engine such that it can meet the powertrain torque demands of the driver.

3.6 Experimental Design

The tests conducted on the engine can be subdivided into three sections: basic performance, system operation, and energy and the environment. These tests are ordered such that it follows the process of getting the engine up and running. This process includes the ability to complete ignition and idle, validation of current data, operation in the system, and finally collecting data to refine further models. These Table 5tests will help meet our main goal and all the objectives to get there. A summary of the tests can be found at the end of this section in Table 6.

3.6.1 Basic Performance

The performanceof the engine must be validated from the original data to assess the use of the engine in the powertrain system. The engine must first be operable and be able to complete ignition, idling, and stopping stages to demonstrate the basic performance and validation of data.

Once the engine is capable of idling, further steps can be employed to test the engine's performance. During the basic performance, an effort to understand the capabilities of the engine. To validate the information, a select set of efficiency points from modeled equivalent engines are tested. Once the data is validated a comparison of the data can be made and the engine can be tested using E85 fuel. The two data sets are then compared and contrasted to validate the design decision to run E85 fuel.

For the basic engine operation only basic information is collected. The fuel injector timing, ignition timing, starter motor, and throttle are all used as input variables to get the engine to start

at idle. The idling speed and time are recorded to see how quickly the engine can be brought online for integration in the system operations.

3.6.2 System Operation

There are two major aspects that need to be considered for the engine operation in the system. To determine the operational potential of the engine in the vehicle, tests that focus on system operation are employed. These include the speed at which the engine can reach the desired rpm and the overall performance that the engine can contribute to the system.

Within the system, the engine can be decoupled from the pre-transmission motor powertrain using a clutch. As the engine is not always operational, it must quickly match the speed of the rest of the powertrain to ensure smooth engagement for the consumer. To test the response speed of the engine, the transient time to steady state speed must be measured to different rpm from rest.

During the parallel mode, the engine is often used at maximum power to aid in the acceleration of the vehicle. The power curve of the engine is therefore of great importance to the team. The specifications of the engine show that it can perform up to 92 kW with E10. The performance of the engine with E85 must, therefore,be tested. The development of a new power curve for E85 fuel is, therefore, essential to determine the amount of power the engine can contribute to the system.

To measure the system performance and validate previous data the team will examine key engine variables as inputs and outputs. For the MPE850, the injector timing, ignition timing, and throttle position will be used as inputs to move the engine to specific operational points. To then measure the performance the time to reach steady state will be examined in addition to torque, speed, fuel consumption, and temperatures from exhaust gas temperature sensors installed on the exhaust manifold.

3.6.3 Energy and Environment

The final test conducted on the engine is on the efficiency of the engine. The test is most important for us as it is not an engine certified for use in a vehicle. The unique use means that the

Energy Protection Act (EPA) certification does not include any automotive application and can only be used under specific exemptions granted by the government of Canada.

As energy consumption and emissions are two large aspects of the competition, accurate data is required. The scope of this paper is however just basic operation, and therefore, optimization is not included in the paper. The focus is just to obtain initial results by running the engine on E85 and E10.

By first running the engine on E10 we will be able to see how the engine operates with conventional fuel. Though the speed of the engine can be higher than 5000 rpm, the pre-transmission motor limits the speed and so only speeds under 5000 rpm are considered. Thespeed limit, therefore, demonstrates the entire operational range of the engine in the powertrain system.Once a baseline efficiency map is created, the tests will be completed using E85 fuel.This testing gives the performance of the engine under the desired fuel and operational range. As E85 has different combustion characteristics, some tuning is required however minimal time will be dedicated as optimization is not a focus as previously mentioned.

Once energy maps have been created for the different fuels, they will be compared and contrasted. This comparison demonstrates not only how the performance characteristics changes but also validates the reasoning for the fuel choice.

Table 6: Summary of tests to be conducted on the MPE 850 engine to ensure operational potential in the vehicle powertrain

Test	Description	Input	Output
Start/Stop	Starting the engine and reaching the idle speed at which a minimal torque that approximates motor inertia is reached	Fuel injector timing, Ignition timing, Starter Motor, Throttle	Engine control signals, Torque, RPM, ΔTime
Steady-state Performance	Test the engine at a set of steady state operating points. The points will be selected to test optimal efficiency points through a number of power bins, and the idle point. (Note: Transients)	Fuel injector timing, Ignition timing, Throttle	Torque, RPM, Fuel Consumption, Temperature
Speed Matching	Test the time it will take for the engine to match a given speed (Note: Transients, Non-Linearity)	Fuel injector timing, Ignition timing, Starter Motor, Throttle	Torque, RPM, ΔTime, Fuel Consumption
Maximum Acceleration	Find the new power curve	Fuel injector timing, Ignition timing, Throttle	Torque, RPM, Temperature

Efficiency	Develop complete efficiency maps for the engine and the resulting GHG emissions	Fuel injector timing, Ignition timing, Throttle	Torque, RPM, Fuel Consumption

3.6.4 Experiment Assumptions and Limitations

There are many assumptions in this work that may limit the accuracy of the data. Many of these assumptions are due to the limitations of the test bench set up that influence the performance of the engine and the data that can be collected. The first assumption in the data is that our cooling is sufficient for both the engine and intercooler. We know this not to be true due to the limitations of while staying static in an enclosed workspace. The biggest assumption, however, is that the engine will operate the same on the bench as in the system. There are multiple external factors that could affect this and therefore, will be the focus of later works and stages of the competition.

The main goal of this work is to improve the modeling. However, there are many differences between the test in simulation and on the test bench that can influence the final results. The modeling allows for continuous operation of the engine at a given speed, but the engine dynamometer can only operate for 15 min before the water is too hot to continue testing. The testing was, therefore, to determine operational performance at given a given point for a minimum 15 seconds to ensure steady state and modeled the performance of the engine at this point for an entire drive cycle.

The bench test set-up also focuses more on the objectives of the paper while the modeling focuses on the end goal. The test bench setup is designed to validate and collect data on the MPE850 engine with both E10 and E85 fuels. This test bench allows the team to meet all objectives. By meeting the objectives, the team can then utilize the validated data to model the vehicle and determine the characteristics of the two control strategies to make a conclusion. This clear distinction between objectives and goal is, therefore, important to note when examining the bench test experimental design and modeling and control analysis.

3.7 Results

Through bench testing the MPE850 engine, various experimental objectives were met. The engine ran using both E10 and E85 to demonstrate not only the performance of the component in the powertrain but also the specific fuel that will be employed on the final vehicle. Results from

the bench test include DYNOmite dynamometer data and data outputted from the MoTeC M400 ECU.

3.7.1 Start and Idle

With the dynamometer setup and the engine fully integrated, one of the first tests performed upon the engine is a startup test. Figure 15 below shows the engine RPM and output torque during a startup procedure. It can be seen that the engine output overshoots before reaching a steady state performance after 12 seconds. With this data collected the HSC can be developed to appropriately start and stop the engine without unanticipated speed or torque increases.

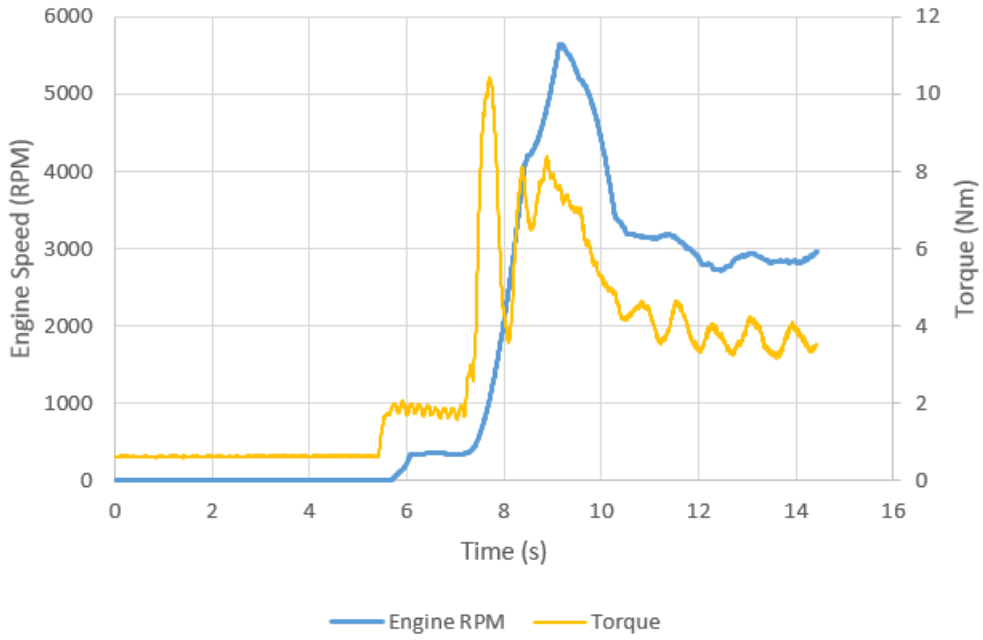

Figure 15: E85 Start and Idle Speed and Torque

3.7.2 Steady State Performance

Steady state performance is achieved through a pulsed width modulation upon fuel injection, developed from the base engine tuning map. Shown in Table 7 is the pulse width and torque developed for different cases and rotational speeds. These results demonstrate the specific speeds and torques can be specified in the design for testing.

Table 7: Toque and pulse width modulation to demonstrate steady state control of engine

	Low Torque		Medium Low Torque		Medium High Torque		High Torque	
	Torque (Nm)	Pulse Width (ms)	Torque (Nm)	Pulse Width (ms)	Torque (Nm)	Pulse Width (ms)	Torque (Nm)	Pulse Width (ms)
2400 rpm	12	3.5	35	5.75	48	7.7	60	9.25
3200 rpm	10	3.45	35	5.67	48	7.59	60	9.12
4000 rpm	12	3.75	35	5.7	48	7.3	60	8.9
4800 rpm	10	3.6	35	5.8	48	7.2	60	8.2

This is most important for controls as it means that specific inputs can be specified to achieve the desired output. In the case study of a vehicle traveling at highway speeds, the torque and engine speed required can be specified as a desired output and the appropriate inputs can be determined. This important step in engine data collection is extremely valuable for engine control and the determination of different control strategies.

3.7.3 Speed Matching

The engine must be capable of quickly getting up to speed to speed match the other powertrain components and work properly as a system. Figure 15 shows that the engine takes 3.5 s to start and reach 5000 rpm. It can be seen however that 2 s are required to start the engine and 1.5 s are required to achieve the appropriate speed.

The startup sequence is not optimized and this time can be greatly reduced. With proper tuning, the engine start up time can be greatly reduced, reducing the 2 s time currently seen. Also the engine could be already idling if required and only the speed matching would be required. This has the potential to reduce the speed matching time to less than 1.5 s and keep the performance feel required in the vehicle.

3.7.4 Performance Curves

The power and torque curves for the MPE850 engine are generated from data collected from the DYNOmite dynamometer. The data is collected and charted to view the bench tested power and torque curve. The results show how difficult it can be to tune an engine and that a lot more effort is required.

The power curve shows a maximum power of 32 kW at 4000 rpm, Figure 16. The data sheet provided shows that at 4000 rpm the engine should be capable of provided approximately 55 kW. The power obtained on the test bench is therefore only 58% of the power the engine should be capable of providing. As stated in the assumptions however it is known that there is inadequate cooling of the engine and a non-functioning intercooler. With these two items operational the power will be higher. Also power can be increase by modifying the air to fuel ratio and the ignition timing. By spending more time tuning a higher power result can be created.

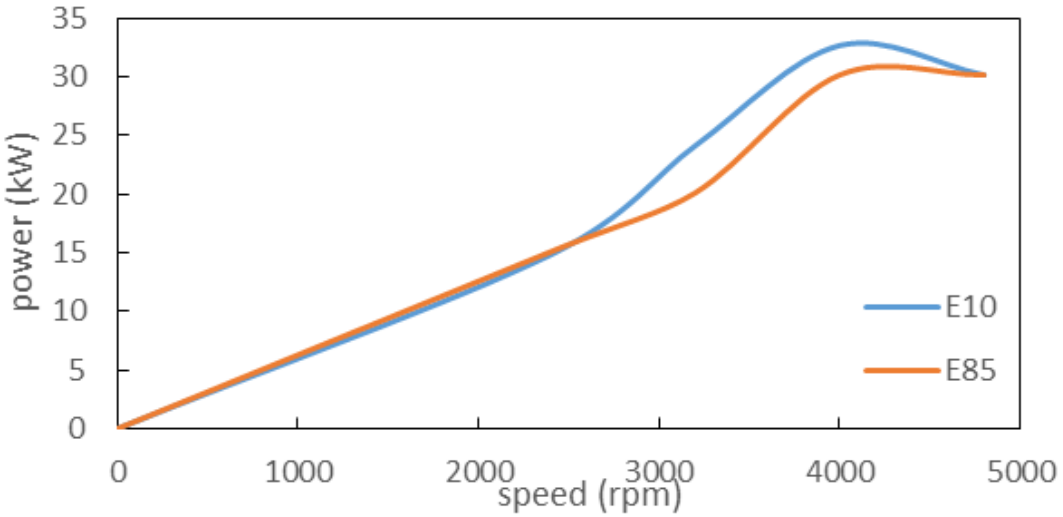

Figure 16: Power curve of the MPE850 engine with both E10 and E85

The power difference between E10 and E85 is minimal as shown above. With only a 2 kW difference more tuning would allow for an increase in power. With proper tuning the result will be much closer the specification data and a marginal difference between E10 and E85 will be created.

The torque curve,Figure 17, also shows a much lower maximum torque than the engine specifications. The maximum torque was found to be 78 Nm for E10 and 72 Nm for E85. This is approximately 65 % of the specified value. Again due to a lack of optimization the torque results can be increased by tuning and modifying the air to fuel ratio and the ignition timing.

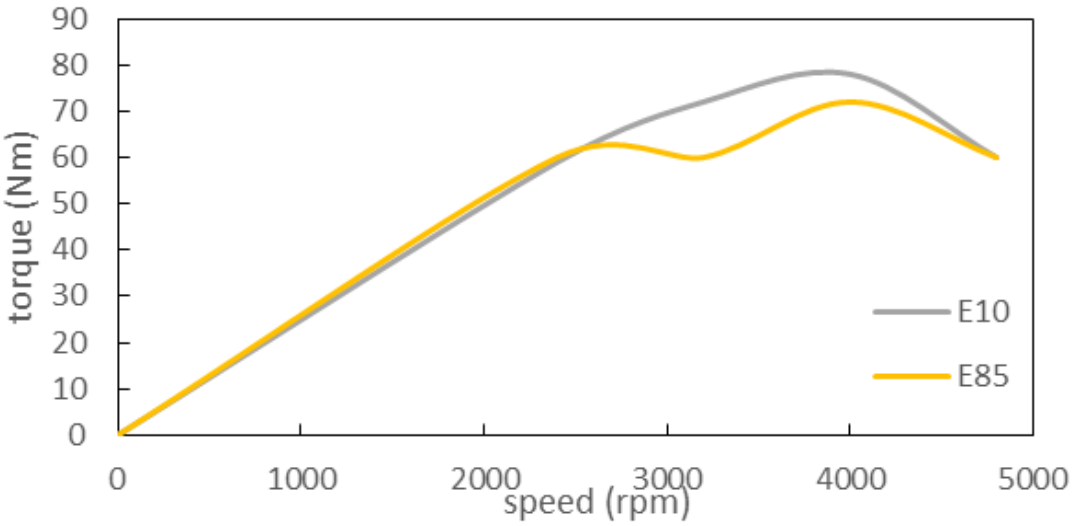

Figure 17: Torque curve of the MPE850 engine with both E10 and E85

3.8 Energy and the Environment

To investigate the efficiency of the MPE850 engine, UWAFT gathers a series of dynamometer test data points which are interpolated into a lookup table to produce an efficiency map. The map, seen in Figure 18, shows that the peak efficiency of the engine is 22%, occurring at 5000 RPM and 70 Nm.

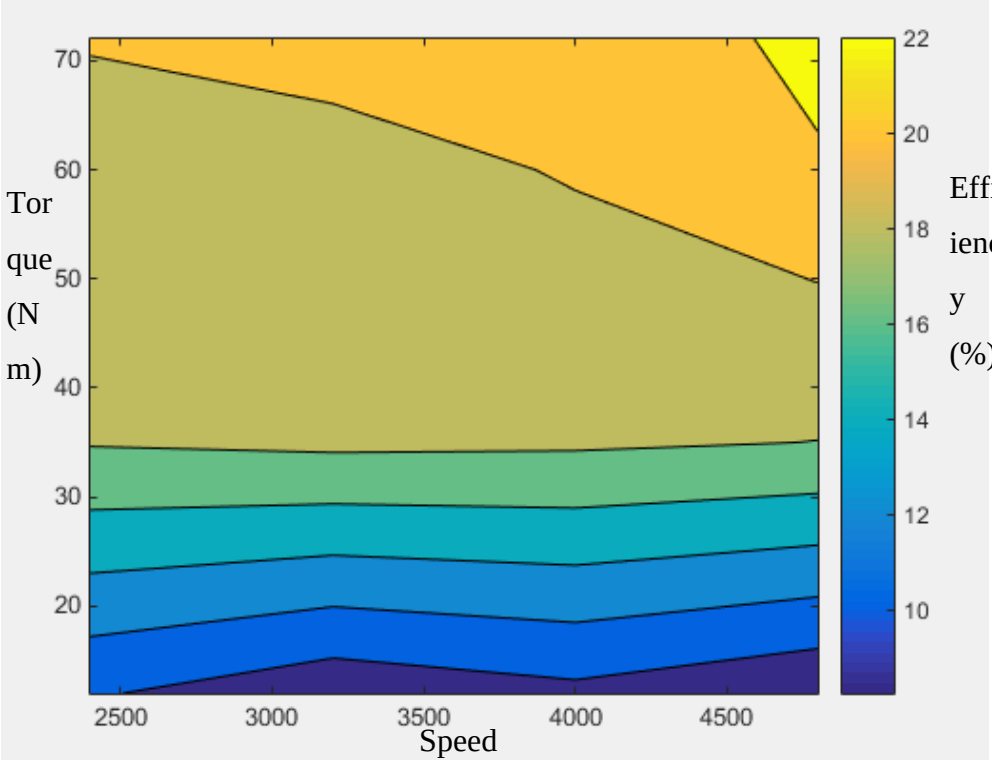

Figure 18: Efficiency map of the MPE 850 engine with E85 fuel

UWAFT acknowledges the peak efficiency is less than that achievable on similar platforms, approximately 35%, and that there is room for improvements in the form of aforementioned engine maps beyond the base efficiency map. In particular, UWAFT anticipates improvements from the development of an ignition timing map to correct for the Ethanol fuel used.

Analysis

Through analysis of the gathered dynamometer data, the authors can validate previous works [29] which aimed to approximate the vehicle acceleration, consumer feel, and energy and emissions of the vehicle.

The full vehicle model generates results used to compare the two control strategies. The vehicle runs at 100 kph 110kph and finally 120 kphthese three speeds approximate highway driving in Canada. In a parallel control strategy, the direct coupling between the engine and the road creates a steady state engine operation once the vehicle speed levels out, see Figure 19. In series operation the engine is at the same operation point for all speeds, see Figure 20. This operation point is a combination of the generator and new-engine efficiency map, isolating the peak efficiency operation point.

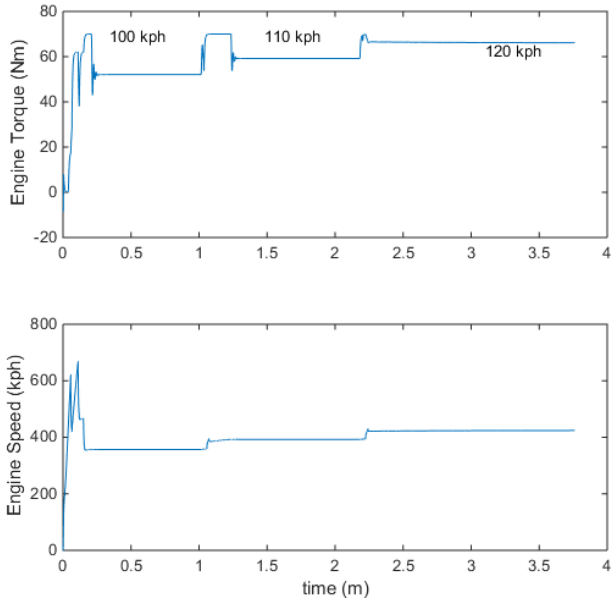

Figure 19: Parallel Operation on Ethanol 85%

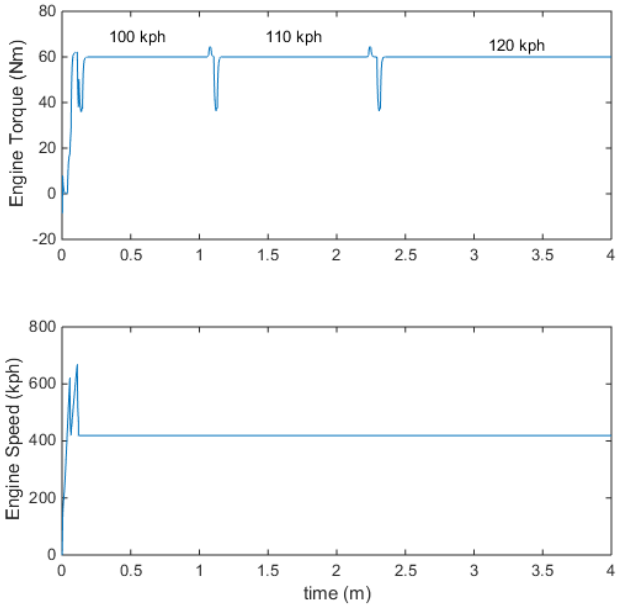

Figure 20: Series operation on Ethanol 85%

The dynamometer tests of the engine are used to determine the efficiency results for all the steady state operations of the engine, illustrated in Table 8. The series operation efficiency out performs the parallel operation at the two slower highway speeds, though at the fastest highway speed the parallel operation is more efficient.

Table 8: Efficiency Analysis of Engine during Highway Operation

	Speed (rad/s)	Torque (Nm)	Efficiency (%)
120 Parallel	423	66	20.47
110 Parallel	392	59	19.88
100 Parallel	357	52	19.26
All Series	419	60	20.08

Figure 21 shows the battery state of charge (SOC) of the test results. At 100 kph and 110 kph the series operation nets a positive SOC but at 120 kph it nets a negative SOC. This would allow the vehicle to run in charge sustaining at a thermos static operation in the first two speeds, but not at the highest speed. Additionally both runs show SOC drops at the speed changes this is due to the electric energy used to accelerate the vehicle for higher performance, and is expected.

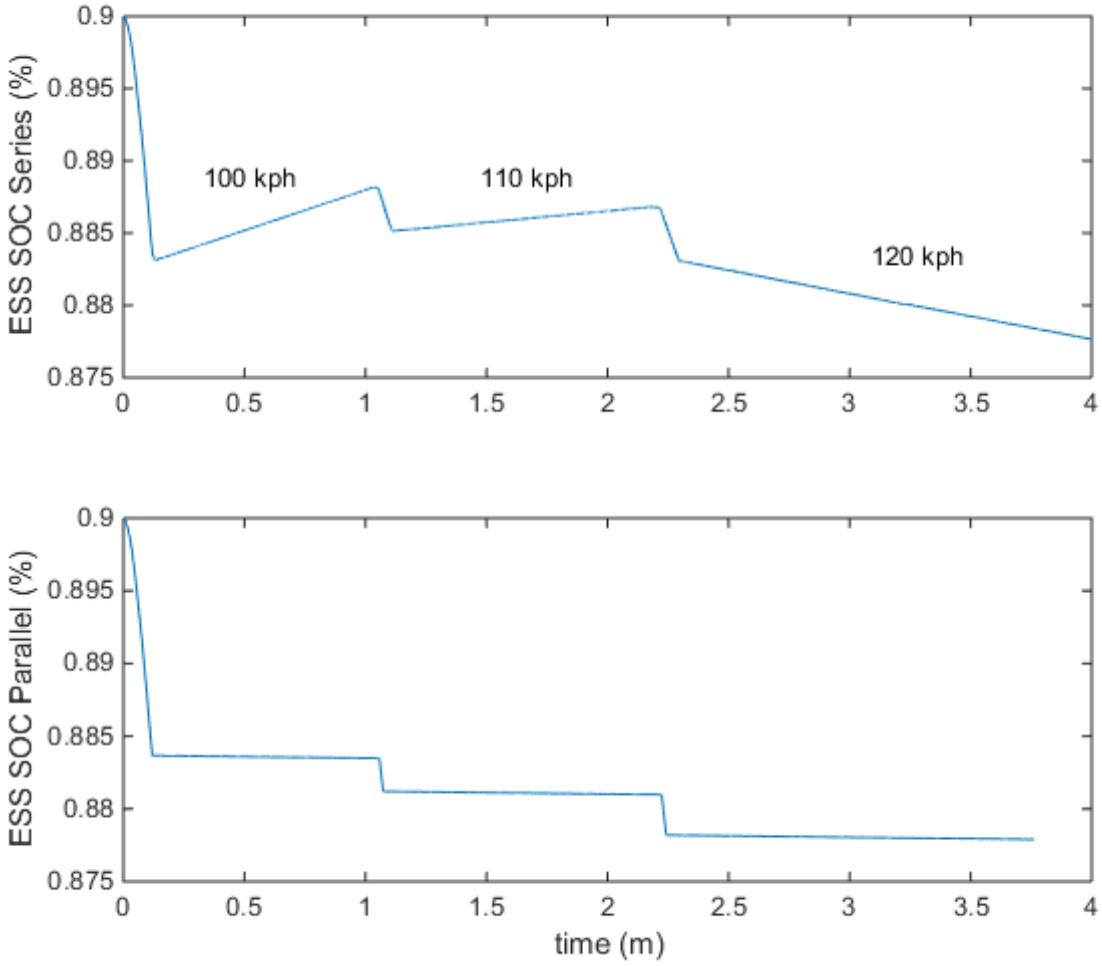

Figure 21: Comparison of Series and Parallel ESS SOC

3.9 Conclusions and Recommendations

UWAFT is able to achieve basic functionality and control of the MPE850 engine through dynamometer testing and has increased the modeling fidelity to examine the effectiveness of series and parallel control strategies. Basic functionality and control is achieved through the start and idling of the engine using a MoTeC M400 ECU and through operation of the engine at a set of fixed speeds and torque requirements. The team showed that further tuning is required as only 58 % and 65 % of the specification power and torque respectively are achieved. Through examining the speed matching capabilities and the engine output performance, the vehicle model is enhanced with actual engine data to determine if the engine can meet the needs of the hybrid

vehicle as designed. In analyzing this updated vehicle model, it is found that the engine is capable of producing sufficient output power to meet highway speed performance requirements. Finally, by comparing a series and parallel control strategy for top highway speeds, it is found that parallel is the most efficient control strategy to employ. UWAFT acknowledges that at lower speeds further analysis is required to determine the optimal strategy for vehicle control.

Chapter 4

Optimizing Vehicle Operation with Pre and Post Transmission Motors

The following section is based on previously published work "Control Analysis for Efficiency Optimization of a High Performance Hybrid Electric Vehicle with Both Pre and Post Transmission Motors," SAE Technical Paper 2016-01-1253, 2016, doi:10.4271/2016-01-1253.byEllsworth et al. [29] This thesis author specific contribution to this paper was to: develop the model, conduct the simulations, prepare graphics and results, prepare the final manuscript and reviewer edits with direction and assistance from the project supervisors and research colleagues who were co-authors.

Control of a transmission generally becomes more complicated when examining PHEVs in comparison to Electric Vehicles (EVs), as PHEVs utilize an additional range extending energy source. There is an additional control system complexity increase as PHEVs have both Charge Depletion (CD) and Charge Sustaining (CS) modes of operation. Many optimization challenges exist specifically to maximize the performance and energy efficiency on a vehicle scale. In this chapter, the control system for a parallel-split PHEV is examined in the context of a vehicle development competition. The University of Waterloo Alternative Fuels Team (UWAFT) is participating in the EcoCAR 3 competition, sponsored by General Motors and the U.S. Department of Energy.

4.1 Competition Vehicle Design

UWAFT is developing a split-parallel architecture, featuring a Weber MPE 850cc turbo-charged engine, two GKN AF130-4 motors, and a 16.2 kWh A123 Energy Storage System (ESS). One motor is located in the pre-transmission position (designated as ‘P2’), and one motor is located in the post-transmission position (designated as ‘P3’). UWAFT has chosen to integrate a clutch between the engine and P2 motor; which, allows the P2 motor to disengage from the engine and this allows the vehicle to run in an all-electric mode, using both electric to power the wheels. A diagram showing the powertrain architecture of the car can be seen in Figure 22. This architecture allows for a series, parallel, or all-electric mode of operation, enabling the control system to select the mode which is most efficient given the drive profile or performance demand.

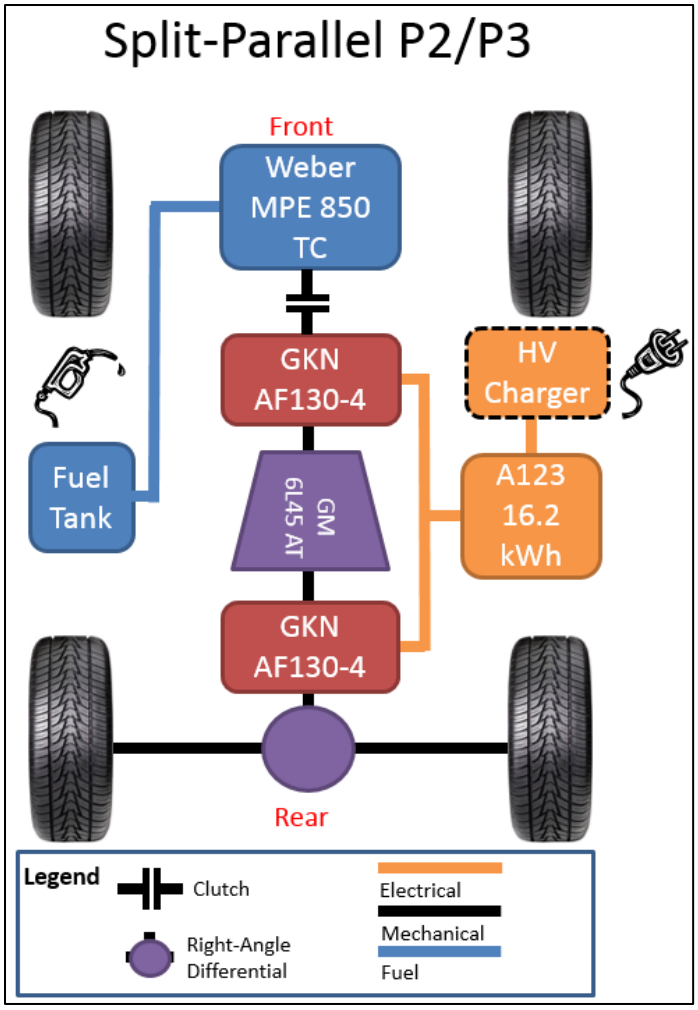

Figure 22: UWAFT Powertrain Layout

The vehicle control system for the selected powertrain can be divided into two groups: industry component control and supervisory control. The industry component controllers onboard the vehicle are developed by the manufacturers themselves, while the supervisory control is developed by UWAFT. UWAFT's supervisory control strategy will coordinate the overall vehicle operation to control and collect feedback from individual component controllers and to guarantee the vehicle's safe operation.

At a high level, there are two primary operating modes of the vehicle – Charge Sustaining (CS) mode and Charge Depletion (CD) mode.

CD mode is employed when the battery is above the minimum State of Charge (SOC). It aims to use the electric energy stored in the battery to propel the vehicle through the electrified

powertrain. Some utilization of the internal combustion engine is permitted in this mode, however it is limited to providing torque-injection during high performance scenarios.

CS mode is employed when the battery depletes below a certain threshold which is often a predetermined SOC. At this stage, the engine is employed to provide the energy needed to propel the car. There are two ways the vehicle can operate in CS mode. The first method has the engine/motor clutch engaged with the transmission in neutral. This allows for series operation with the P2 motor and engine maintaining the SOC of the battery and the P3 motor providing tractive torque to the road. In the second method, the engine is directly coupled to the road. It produces an amount of torque greater than or equal to the driver demanded torque, the P2 motor can us any excess torque in a regenerative capacity. This 'regenerating' thus provides current to the battery to maintain the SOC.

4.2 Control Strategy & Modeling Development

UWAFT follows a model-based design approach for controls development. By progressing through the stages of Model-in-the-Loop (MIL), Software-in-the-Loop (SIL), Hardware-in-the-Loop (HIL), and Component-in-the-Loop (CIL) before integrating hardware into the vehicle, the team has the flexibility to modify modeling information and controls while integrating the physical components into the system. Validation is performed at each stage of the development, and should an unexpected development occur, the team can step back in the model-based design process to re-tune the system whilst minimizing the time required to implement these changes effectively. The specific timeline for the team's modeling and controls development over the course of the first two years of EcoCAR 3 can be seen in Figure 23.

The results outlined in this paper follow the model as it transitions from a MIL model with individual component controllers to a SIL model featuring a supervisory controller. The SIL model's supervisory controller emulates the real time control signals, increasing the fidelity of the control scheme. Additionally, as the modeling continues through the process and as more data is collected, the component models increase in accuracy.

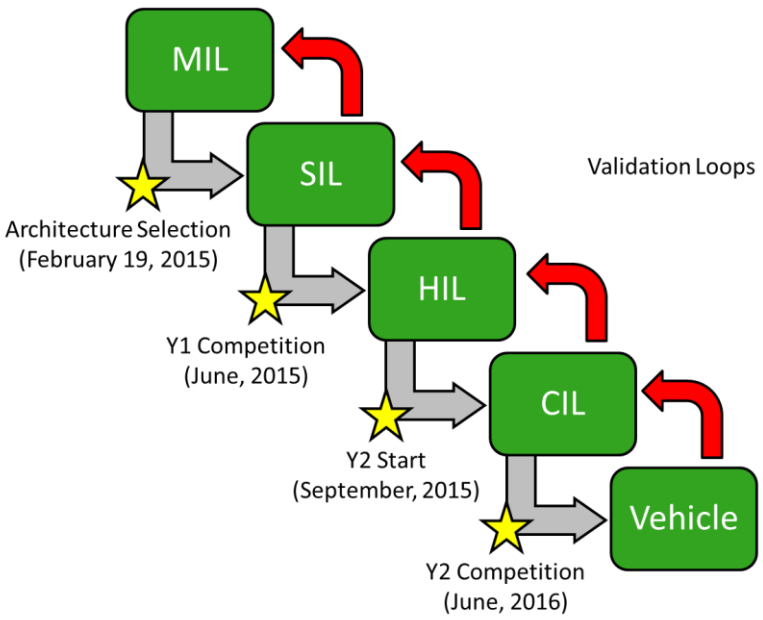

Figure 23: Modeling and Control Development Timeline

UWAFT identified new and innovative technologies to enhance the power of the provided stock vehicle; selecting a small turbocharged engine in conjunction with two axial flux motors to provide propulsive power. Table 1 below presents a high-level summary of the major powertrain components selected in the vehicle architecture.

Table 9: Powertrain Components

Component	Manufacturer/Model	Specifications
Engine	Weber MPE 850cc Turbo	PP: 92 kW
P2/3 Motor	GKN AF130-4	PP: 70 kW (300 V)
		PP: 80 kW (350 V)
Battery	A123 6x15s3p	Cap: 16.2 kWh
		N Volt: 292 V
Transmission	GM 6L45 AT	6 Gear, Longitudinal Auto
Final Drive	GM 3.73 Final Drive, eLSD	3.73 : 1 Final Drive Ratio

Note: PP: Peak Power, PC: Peak Current, CP: Continuous Power, Cap: Capacity, N: Nominal, eLSD: Electronic Limited-slip differential

4.3 UWAFT EcoCAR 3 Camaro Model

UWAFT's modeling efforts in year one of the EcoCAR 3 competition are mainly focused on the use of Autonomie, a vehicle modeling software developed by Argonne National Laboratory. Autonomie is a software wrapper which works with MATLAB and Simulink to automatically generate models within the Simulink environment. UWAFT began its modeling process by using default vehicles and models within Autonomie, relying on component models for items such as engines and motors which are independently validated by the suppliers. UWAFT also generated its own models for additional components which team has proposed for vehicle integration. Additionally, it is noted that UWAFT runs vehicle simulations within the Simulink environment once the initial modeling stage is completed. The developed UWAFT vehicle architecture power flow from Autonomie can be seen in

Figure 24.

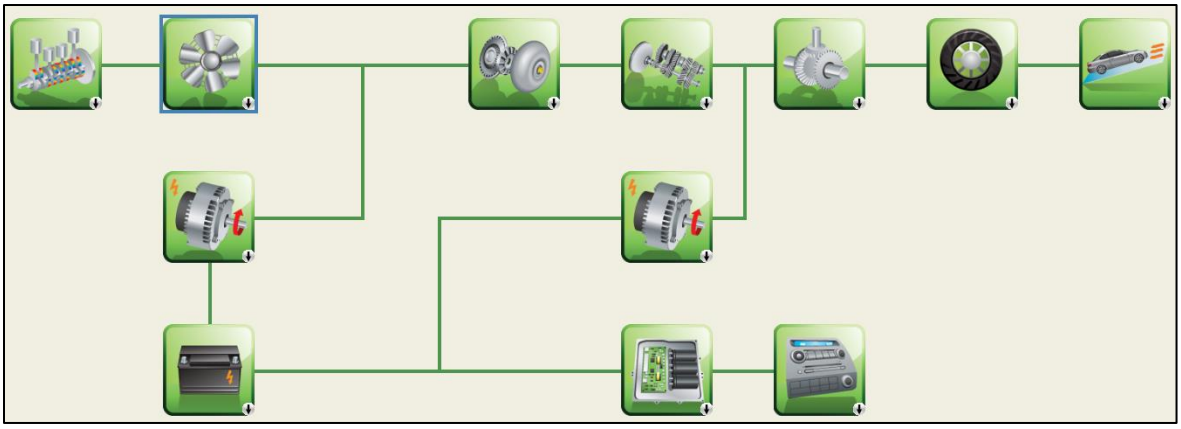

Figure 24: Split-parallel PHEV Powertrain Diagram in Autonomie

4.3.1 Engine

The engine selected for the architecture is a turbocharged Weber MPE850t engine. The selection of a small engine and turbocharger is desirable as the system's energy efficiency extends range while still meeting performance demands [30][31]. This motor has a lower weight and size in comparison to the stock motor and this aspect of the motor system is especially important as it provides space for additional components such as the P2 motor.

As a result of the flexibility of the power flow in the developed architecture, a set of equations that model the engine and the system's power consumption are required. While operating in series mode, the energy efficiency of the engine and P2 motor are maximized through a control strategy which operates the motor in a series configuration. In this manner, the energy efficiency of the engine and P2 motor are maximized, and the control scheme operates such that the engine's peak energy efficiency matches the motor's peak operating energy efficiency. This control scheme maximizes energy generation efficiency whilst applying a thermostatic control strategy. During parallel operation, it is required that the motors and engine are capable of outputting the peak wheel torque and maximizing overall the acceleration of the vehicle. In coupling the output of the Weber MPE850t to the input of the electric GKN motor, power is generated at a near-optimal energy efficiency because of compatible torque and speed curves. This is a key benefit given that there are not many ethanol capable engines in production with energy efficiency curves that correspond to electric motor efficiency curves.

4.3.1.1 Power/Torque

The torque versus speed map for the Weber MPE850t is shown in Figure 25. This engine outputs a maximum power of 92 kW, but due to limits in the coupling with the P2 motor, the engine's output must be limited to reduce counter-electromotive force. This reduced force results in a higher energy efficiency of the powertrain, but limits the power to approximately 60 kW at 4500 RPM.

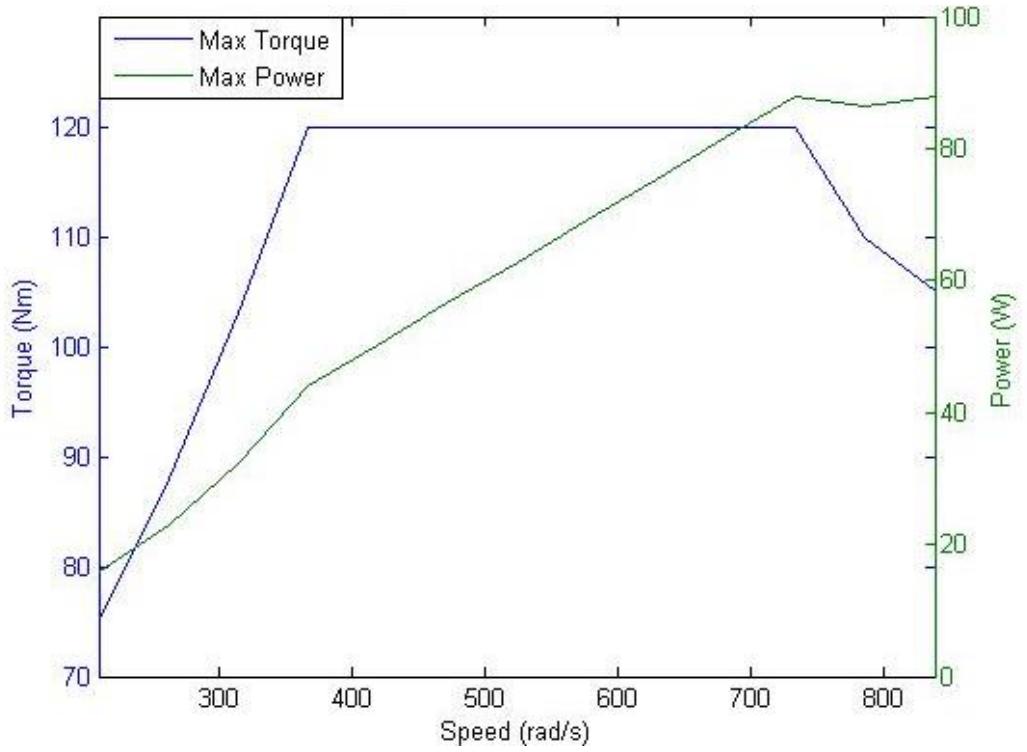

Figure 25: Weber Performance Curve [32]

4.3.1.2 Efficiency map

The engine model uses a fuel rate 2-D lookup table which details the mass flow rate of E85 used at each speed and torque. This map describes how the engine's energy efficiency is calculated in the model. Due to legal issues, the exact energy efficiency map and fuel rate map for this engine cannot be applied in this paper. Instead, an approximation for the fuel rate is made from fuel maps provided by Argonne National Labs. The fuel rates chosen are from a Honda Insight engine model, which is a stock model in Autonomie. This engine model is the smallest provided in Autonomie. It is a 1000cc engine similar in size to the 850cc Weber engine selected by UWAFT. To best represent the engine efficiencies that would be seen by the smaller Weber

engine, the maps are scaled by the torque difference between the two motors, and the resulting fuel consumption map is converted to an ethanol consumption map using a scaling factor. The E85 scaling factor is obtained by comparing the E10 and E85 fuel consumption maps provided for the EcoCAR-sponsored GM LEA engine. The resulting efficiency map describes an engine with a peak efficiency of approximately 41% and can be seen in Figure 26, which has been found to be appropriate for high pressure ethanol engines [33]. While reasonable, using all of these steps leads to inaccuracies providing a coarse approximation of the engine efficiency and is only used due to a lack of high fidelity data.

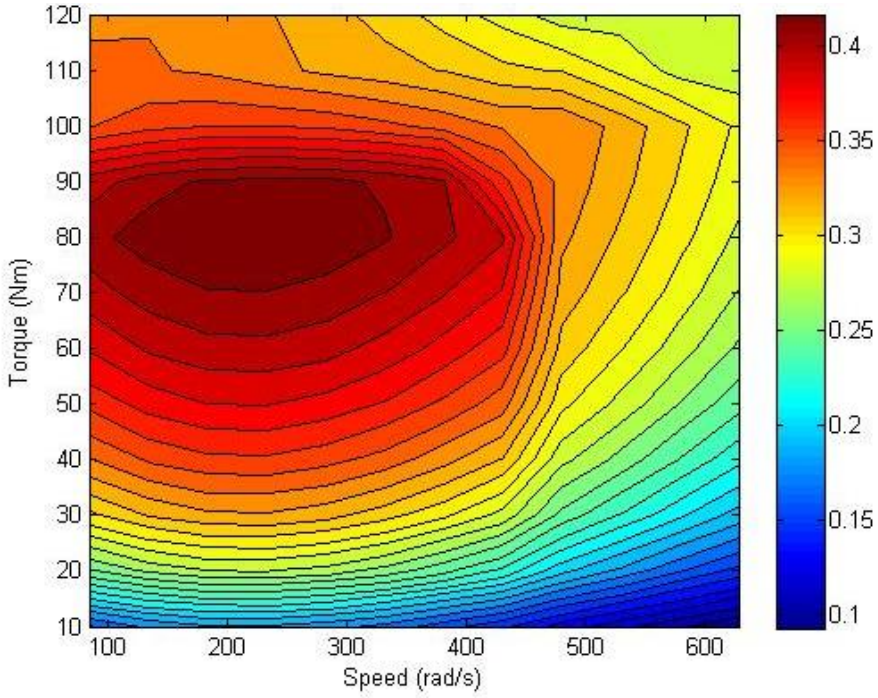

Figure 26: Engine Efficiency Map

4.3.2 Transmission

UWAFT's 2016 Camaro utilizes a GM manufactured transmission (6L45) which enables the engine and P2 motors to operate at their most efficient operating points. The 6L45 is an automatic transmission which is longitudinally mounted in the vehicle. UWAFT's modeled transmission is based upon a stock model found within Autonomie software. UWAFT utilized stock transmission efficiencies in the model and modified the model's gear ratios to reflect those of the 6L45. The developed gear ratios and their corresponding efficiencies can be seen in Table 2.

Table 10: Transmission Gear Ratios and Efficiencies

Gear #	1	2	3	4	5	6
Efficiency	0.96	0.95	0.95	0.98	0.93	0.93
Ratio	4.06	2.37	1.55	1.16	0.85	0.67

There are a number of losses in the couplings of the transmission, most notably in the torque converter. UWAFT intends to keep the torque converter installed for the purpose of simplifying the control system around the transmission. This control system must synchronize the rotational speed at the input and output of the transmission during gear shifting operations. The transmission's torque converter is most efficient at high-torque, low-speed scenarios as seen in Figure 27.

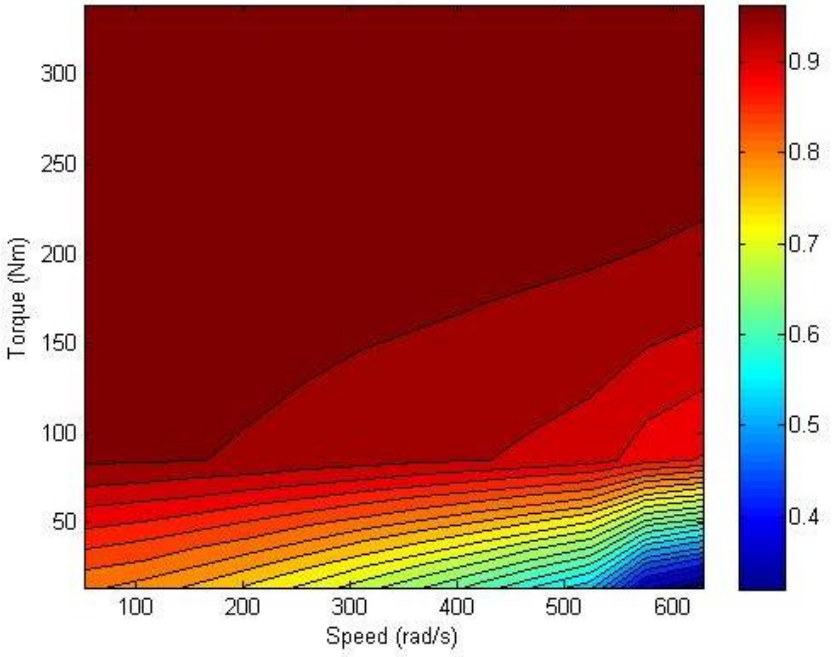

Figure 27: Torque Converter Efficiency Map

4.3.3 Motor

There are two axial-flux, permanent magnet motors selected for use in UWAFT's EcoCAR 3 Camaro architecture. These motors are manufactured by GKN and are packaged in an extremely compact enclosures, aligning well with the space and weight objectives of EcoCAR 3. This motor packaging also aligns well with the EcoCAR 3 competition as it involves a mechanical shaft throughput option for improving rear-wheel drive performance alongside requiring minimal

additional packaging to enclose power sources. It is noted that rear-wheel drive is an EcoCAR 3 competition requirement.

4.3.3.1 Power/Torque

One of the biggest benefits of using electric motors for vehicle propulsion is the ability to use all of the motor's available torque at low speeds. This output torque is sustained throughout the motor's speed range until a peak power is attained. In the UWAFT Camaro, an A123 battery pack is chosen which will keep the vehicle's high voltage bus at a nominal voltage of 292 volts. The resulting GKN AF130-4 power versus torque curve used in the 292 volt model is included in Figure 28.

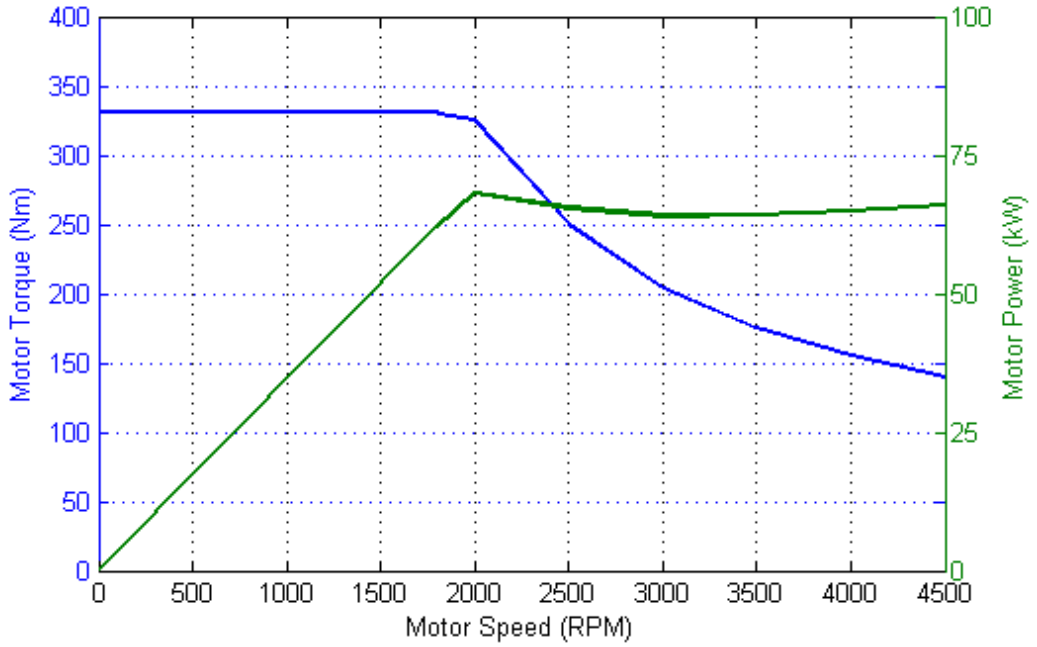

Figure 28: GKN Power/Torque Curve

4.3.3.2 Efficiency Map

The electric motors run at a significantly lower rpm than the traditional electrified vehicle motors due to their unconventional flat cylindrical design. These high torque, low speed motors have their highest energy efficiency operation close to their peak speed, at low torque operation. Due to non-disclosure agreements between UWAFT and the motor manufacturers, exact efficiency maps cannot be included in this paper, but are used in the modelling.

4.3.4 Energy Storage System

The Energy Storage System (ESS) model uses the basic Internal Resistance (R_{INT}) model to approximate the internal resistance of the battery and open circuit voltage of the battery. The R_{INT} model correlates the battery's operation to a single resistor. This model is characterized by the application of a modified Hybrid Pulse Power Characterization Test (HPPC), characterized in tests carried out by UWAFT team members. These HPPC tests are performed on half-cells of the architecture's selected A123 battery. In the conducted testing, the HPPC test curve is modified such that pulses are more indicative of the peak pulses in a real drive cycle such that the results can be extrapolated to represent the full vehicle pack. The current profile for the modified test and its comparative Urban Dynamometer Driving Schedule (UDDS) current taken from the vehicle model is shown in Figure 29.

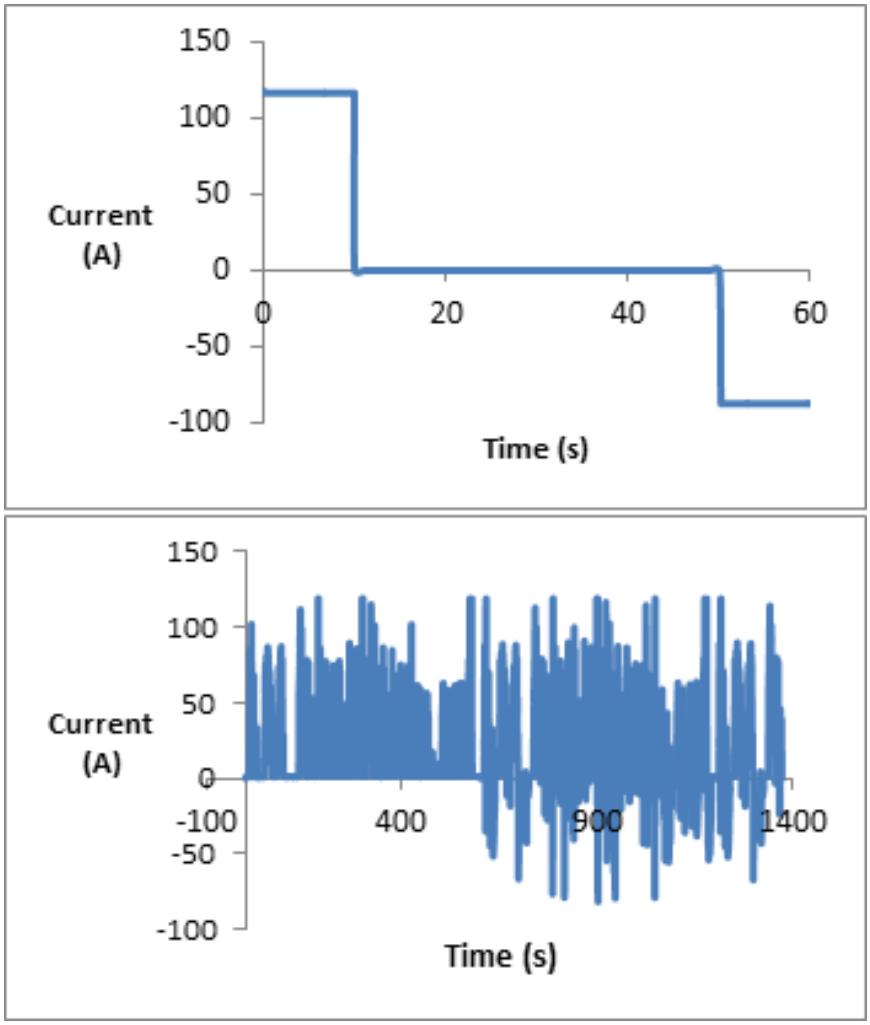

Figure 29: Current profiles for modified HPPC test (top) and Autonomie generated UDDS drive schedule (bottom)

The resulting charge and discharge profiles of the vehicle ESS in the model can be seen in Figure 30. These results are then used in the model to create a higher fidelity battery model that better accounts for battery efficiencies as a function of the SOC.

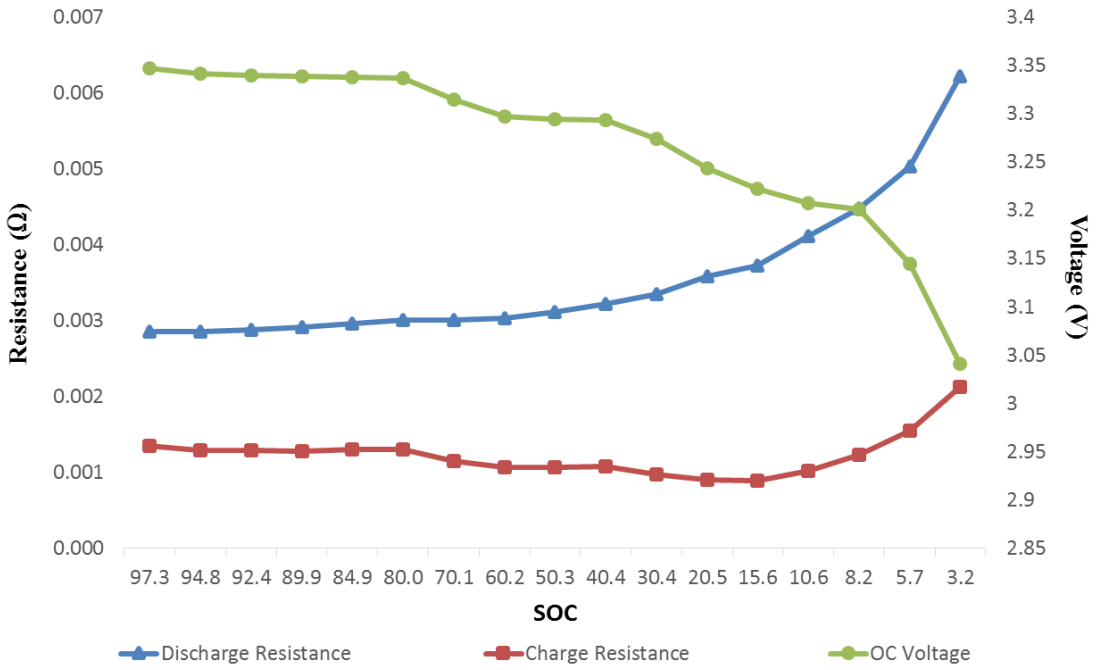

Figure 30: Resistance and open circuit voltage vs. SOC

4.4 Model Limitations

There are many available methods employable to model complex vehicle powertrains. UWAFT has utilized lookup tables and the simple mathematical relations within the structure provided by Autonomie. It is this combination of techniques which addresses both simulation time and memory limitations alongside the scarcity of the available component data.

Lookup tables consist of a discrete n-dimensional space which is parameterized by n coordinates that typically map these coordinates to a single value. For example, a two-dimensional lookup table could map a component operating torque and speed to a value representing the mechanical efficiency at that torque and speed. Lookup tables often provide a good time-memory tradeoff since a small set of points held in memory can be interpolated to yield a value for any input coordinate couple. Additionally, lookup tables facilitate optimization and require no external modifications to the model structure if the lookup table data is modified.

The use of lookup tables and the accuracy they provide heavily depends on the fidelity and accuracy of the data used to create the lookup table. Additionally, a careful assessment of the conditions under which the data was recorded must be made. For example, a "fuel consumption

map" for a warm engine will be considerably different from that of a cold engine. To accurately capture the physics involved in a lookup table, the number of input variables can become very large. Since the required simulation memory is of order n, increasing the dimension of the lookup table space can have a dramatic effect. Engine efficiency for example is a function of many different parameters, but is represented in the model as a steady state value which is additionally simplified to a function of operating torque and RPM exclusively. This type of simplification trades-off potential model accuracy for a reduced memory consumption.

Mathematical modeling is also employed for connecting to and performing calculations upon the lookup maps during model execution. While this approach provides considerably increased accuracy and simulation capabilities, it also introduces complications. One such complication is maintaining numerical stability when the equations of the simulation do not converge to an acceptable solution. Typically, stability issues introduce errors which grow proportionally to the time length of the simulation. Integrator wind up, division by zero, and floating point error accumulation are also common issues. By executing drive cycles compartmentally, the total simulation time is reduced and these types of errors can be managed more effectively.

One of the main limitations of the developed vehicle model is the absence of thermal modeling. The thermal properties of the selected components significantly depend on their location in the vehicle, their proximities to other components, and their physical structure and material of manufacture. It is very difficult to capture these properties into a comprehensive model, especially during the early stages of vehicle development. The thermal properties therefore can only practically be approximated. Alternatively, the model results can be interpreted to be under ideal thermal conditions.

While the model does aim to be comprehensive in terms of the systems it models, many physical aspects of these systems are simplified or approximated. For example, a model of the resonances created by the switching of motor inverters on the high voltage DC bus is not required for the general vehicle model, but could be developed in an external model to evaluate the stability of the bus over the switching frequency ranges of the inverters.

Overall, the primary limitations and approximations within the vehicle model include:

- No thermal management of components.

- No evaluation of transient phenomena such as voltage/current dynamics
- No consideration of degradation and aging effects
- No inter-component interactions such as vibration or thermal conduction which may affect the powertrain energy efficiency
- Power converters operate at nominal input/output values

4.5 Vehicle Modes and Operations

The most significant advantage of utilizing a split architecture is the ability to run in multiple vehicle modes to optimize energy efficiency based upon parameters such as available SOC, and vehicle torque or speed demand. The two distinct modes of vehicle operation are Charge Depleting (CD) mode, and Charge Sustaining (CS) mode.

4.5.1 Charge Depleting Mode

Within the CD mode, there are two main operations that are employed. The first is an all-electric EV operation where either one or both of the motors propel the vehicle with the powertrain decoupled from the engine via the vehicle's clutch. These electric motors utilize the advantage of the gear ratios within the transmission and the final drive to increase energy efficiency. A power flow diagram showing EV operation can be seen in Figure 31.

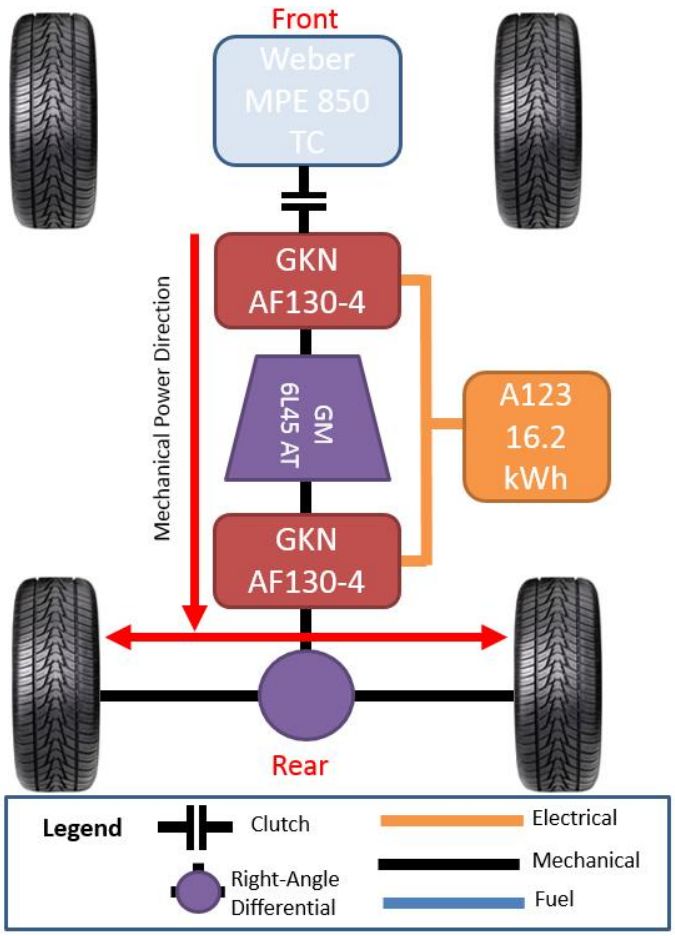

Figure 31: EV Only Power Flow

There is also a performance operation within the CD mode, where the vehicle can couple the engine by engaging the clutch to inject mechanical power into the powertrain should the electrical motors not be able to meet the torque required demand. In this performance CD state, there is an approximate combined power available to the rear wheels of 232 kW; ample power to reach the performance acceleration targets established by UWAFT and the EcoCAR 3 competition. The performance mode power flow diagram is included in Figure 32.

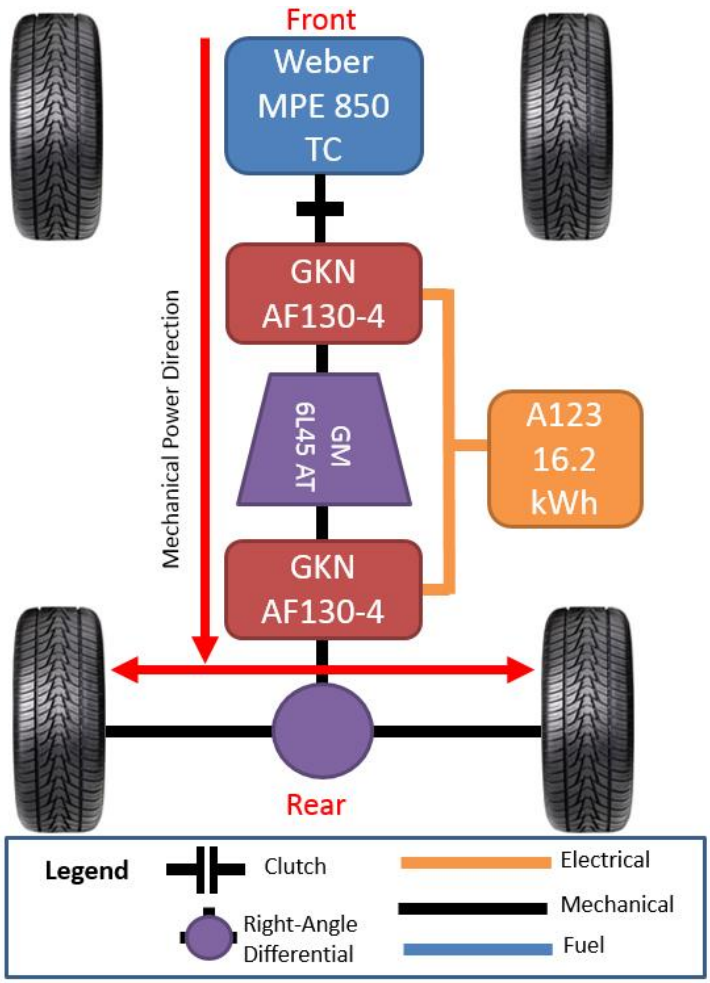

Figure 32: Performance Mode Power Flow

4.5.2 Charge Sustaining Mode

Within the CS mode, there is a series operation, a parallel/performance operation, and an Internal Combustion Engine (ICE) operation. The series operation mode utilizes the transmission as a clutch, and this separates the engine-P2 motor combination from the driveline. From this separation, the engine and P2 motor are able to operate at their peak generation efficiency regardless of driver demand. In series operation, power is transmitted to the tires utilizing only the post-transmission P3 motor. As indicated previously, the Weber Engine and GKN EVO motor have energy efficiency curves which overlap at similar peak speed ranges, thereby optimizing their efficiency when operating in a series mode. The series power flow diagram is included in Figure 33.

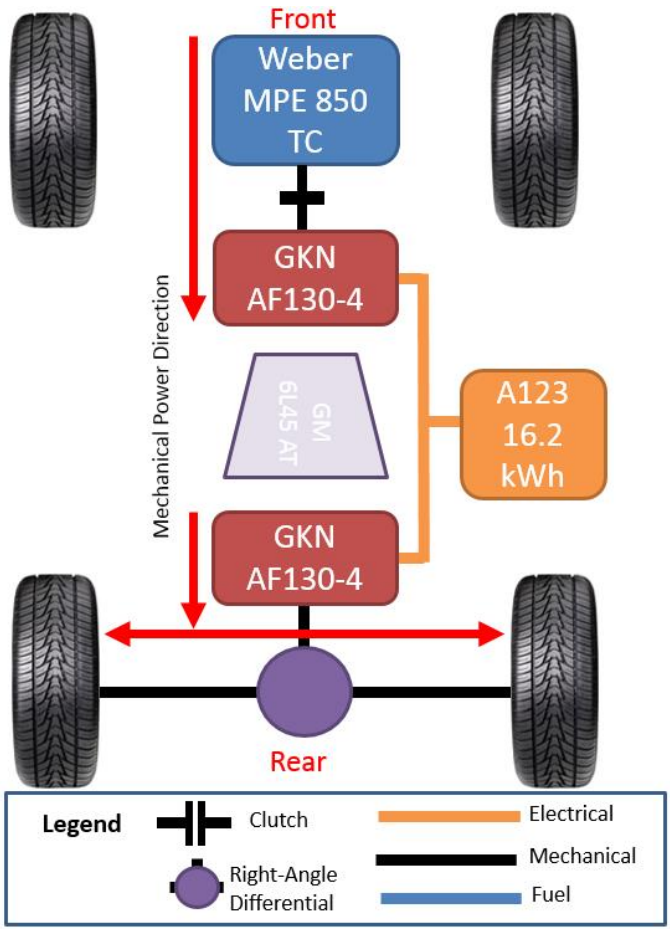

Figure 33: CS Series Operation Power Flow

When the P3 motor alone is not capable of providing enough torque, a parallel or performance operation is employed. The performance CD mode is transitioned to by engaging the transmission and connecting all the power generating components to the road in the same manner as a CD performance mode operation. The operation in CS mode differs from that of CD as one of the motors utilizes a portion of the supplied torque for regeneration, sustaining the SOC. The power flow diagram for this mode is the same as parallel in CD operation, and is shown in Figure 32.

ICE-Only operation solely uses the vehicle's engine for propulsion. This operation mode is the most basic vehicle propulsion strategy, and it will be primarily used as a benchmark for CS mode development as the only charging which occurs in this mode is from regenerative braking. The power flow diagram for ICE-Only operation is included in Figure 34.

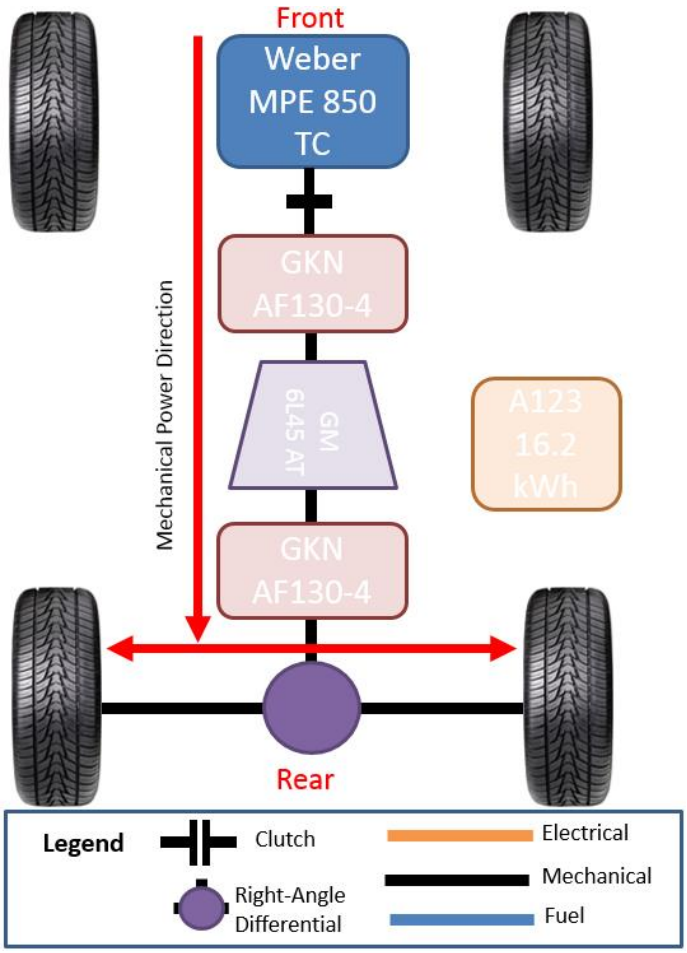

Figure 34: ICE-Only Power Flow

4.5.3 EV Only Control

During EV only operation, the P2 and P3 motors, in addition to the transmission, are controlled by a supervisory controller with the engine clutch disengaged. Using this all-electric operation is extremely favorable due to the high energy efficiency of the vehicle's primary electric components (batteries, motors, and inverters) when compared to that of the combustion engine. In addition to the energy efficiency benefits of using electric components, the vehicle's tailpipe emissions are nullified. Thus, in EV operation, the vehicle itself creates no greenhouse gas (GHG) emissions. It is noted that well-to-pump sources are still a factor when identifying the full environmental impact of this operating mode. This operation mode is then the most effective environmentally when clean electrical power generation methods are utilized. In Ontario, the target demographic of UWAFT's 2016 Camaro, more than 70% the electricity generated is from clean sources [34].

It is important to realize, however, that the ability of the vehicle to run in this EV operation is limited by the SOC of the battery. Recognizing this, the team has sized the battery pack such that the vehicle will achieve the daily average drive distance in EV-only operation before needing to transition into a charge sustaining mode. UWAFT has a modeled EV range of 54.58 [km] which is greater than the average daily drive length of 40.55 [km], identified by Oakridge National Laboratory [7]. Thus, UWAFT applies a maximal energy efficiency operation mode for the entirety of an average driver's route.

4.5.3.1 The Initial Control Strategy for EV

This report explores the difference between two EV control strategies. The first, initial, strategy uses only the P3 motor to drive the vehicle during its charge depleting operation; a control strategy which attempts to maximize energy efficiency given that the P3 motor does not suffer from the losses in the torque converter or transmission. The second strategy is developed in an attempt to further optimize the performance of the system.

This control strategy's energy efficiency and a trace for a 505 cycle can be seen in Figure 35 and Figure 36 respectively. It can be seen that the motor has an efficiency far above that of an engine at all speeds, however, it performs at its highest efficiency when the vehicle is nearest to highway speeds and at a low acceleration demand.

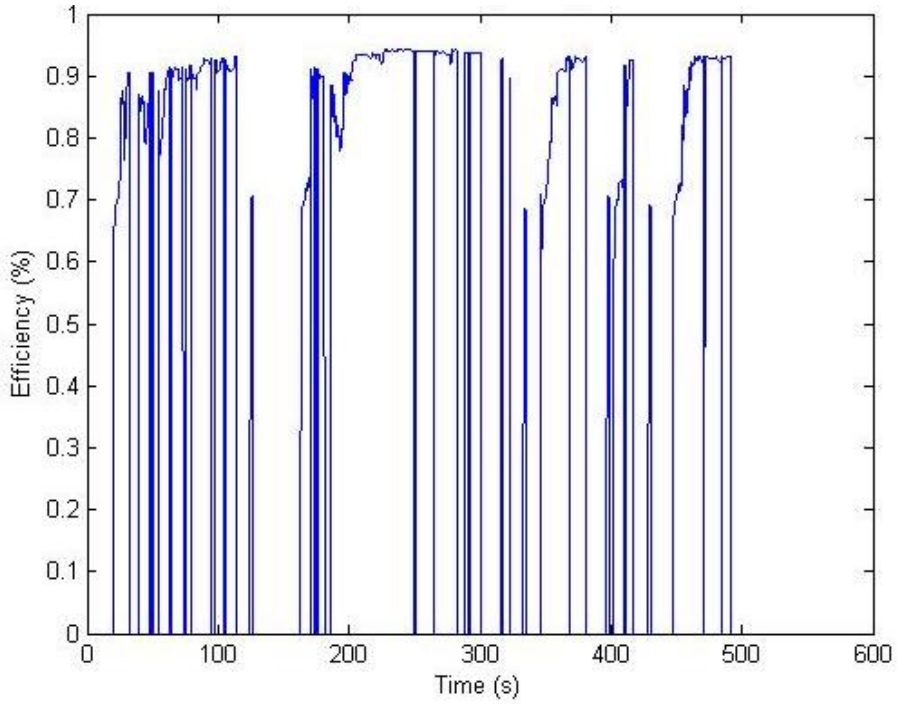

Figure 35: EV system efficiency for simple EV control (505 Cycle)

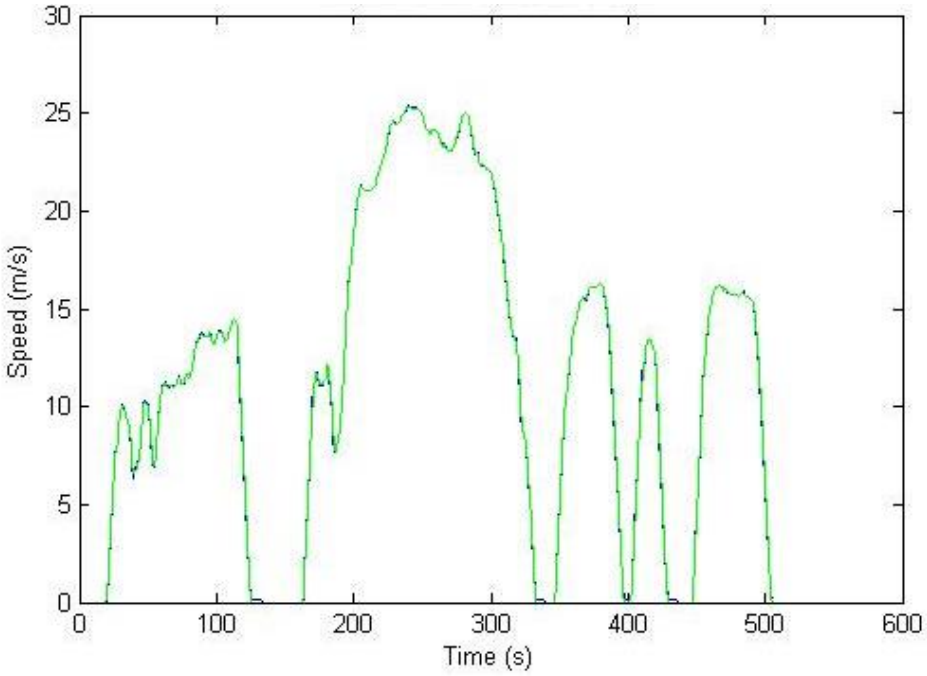

Figure 36: Velocity trace for 505 cycle

4.5.3.2 Optimized EV Control

The second control strategy involves manipulating the electric propulsion demands from the P2 and P3 motors. While the P2 motor has the same efficiency as the P3 when operating at the same motor speed, the dynamic gear ratio of the transmission allows the P2 motor to have higher efficiency at lower linear vehicle speeds. At low linear speeds, the gear ratio of the transmission increases the angular velocity of the P2 motor, and this allows the motor to operate in a range of increased energy efficiency. Additionally, the P3 motor provides more power at higher linear speeds, as it runs more efficiently at higher angular velocities and does not suffer from the energy efficiency loss inherent in the transmission. The P2 and P3 motors thus complement each other in a range of operations to maximize the use of available electrical energy.

There are three variables that need to be optimized for this operation to run at peak energy efficiency: the P2 motor torque, the P3 motor torque, and the transmission gear selection. These variables need to be optimized across the entire range of performance demand and vehicle speed. The performance demand from the driver is represented in many different forms throughout the model, but the most significant frame for this purpose is the torque requested at the wheels. As such, the optimization will utilize two lookup tables. The first takes the wheel torque demand alongside the linear speed of the vehicle and outputs the percentage of the demanded torque to be satisfied by each motor. The second takes the same two inputs in addition to a wheel torque demand and linear speed, and then outputs the transmission gear selection.

These look up tables are developed using a script within MATLAB that compares all the energy efficiency maps of the involved components (P2 Motor, P3 Motor, Gear Coupling, and Torque Converter) throughout the entire range of operation, where all possible iterations of each control variable are considered. The process for this comparison would effectively output one hundred efficiency maps for each of the six gears, one for each percent change of P2 to P3 torque (torque split). These maps are then compared against each other, with the maximum energy efficiency taken from each. The optimized map that is created is shown in Figure 37. For each wheel torque request, the maximum efficiency, gear and torque split are mapped and can be seen in Figure 38, and Figure 39.

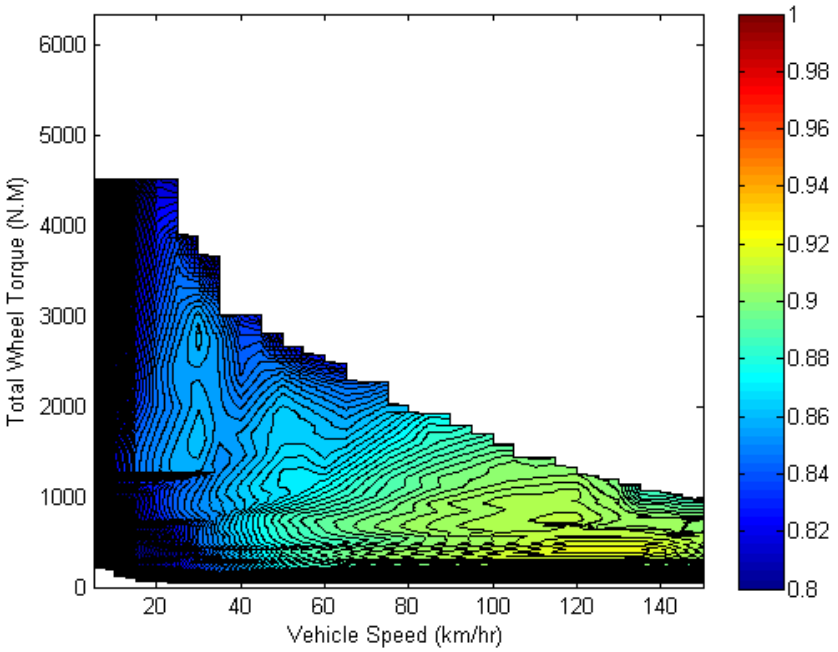

Figure 37: Powertrain peak efficiency during EV operation

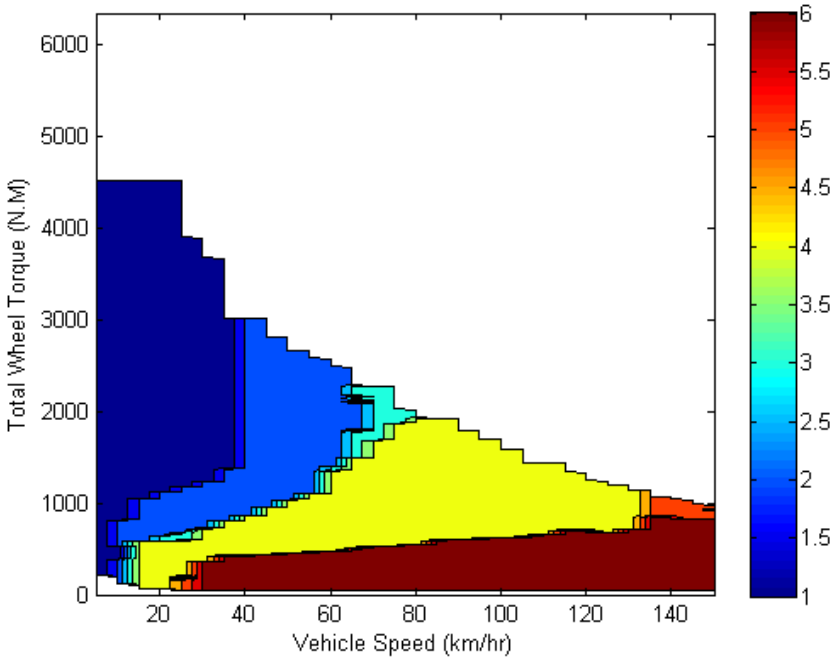

Figure 38: Gear selection for optimized efficiency during EV operation

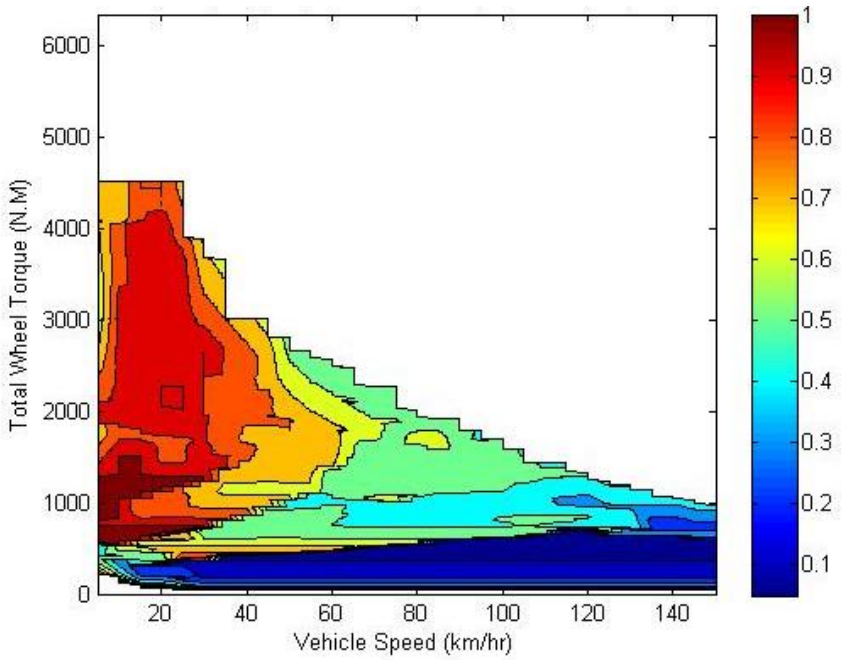

Figure 39: Torque Split for optimal efficiency between P2 and P3 motors during EV operation

Figure 40, compares the energy efficiency of the original EV control strategy to that of the optimized strategy for the 505 cycle. The two-motor EV operation shows a significant increase in energy efficiency, specifically at points where the vehicle is requiring large accelerations at non-highway speeds.

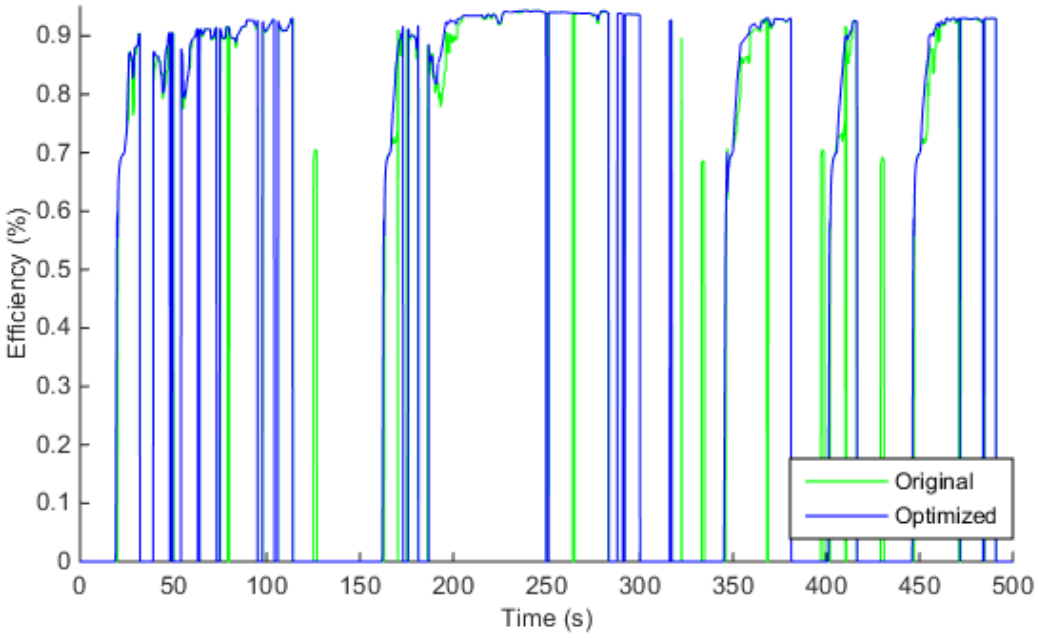

Figure 40: EV Efficiency after optimization compared with original

4.5.4 Charge Sustaining Control

During Charge Sustaining mode, the vehicle attempts to maintain the SOC at a steady value. The power generation required to keep the SOC steady will involve the use of the engine as a range extender. In this report, two engine control strategies will be evaluated.

4.5.4.1 Initial Control Strategy for Charge Sustaining

The initial charge sustaining mode runs the vehicle as a standard internal combustion engine vehicle, satisfying all demand torques with the engine. There are two notable exceptions to this rule however: the vehicle will still regenerate power through the motors during braking, and, if the power demand is above the performance threshold, the vehicle will still use the motors to inject power. This operation results in an energy efficiency that is non-optimal as the engine efficiency is extremely volatile based on torque and speed.The 505 cycle velocity trace and the engine efficiency for this initial control strategy during the 505 cycle can be seen in Figure 41, and Figure 42. The engine must provide all the propulsive power for the vehicle in this operation. Additionally, since the engine is coupled to the road, it has limited options for rotational speed. The resulting highly fluctuating drive efficiency is seen in the efficiency cycle.

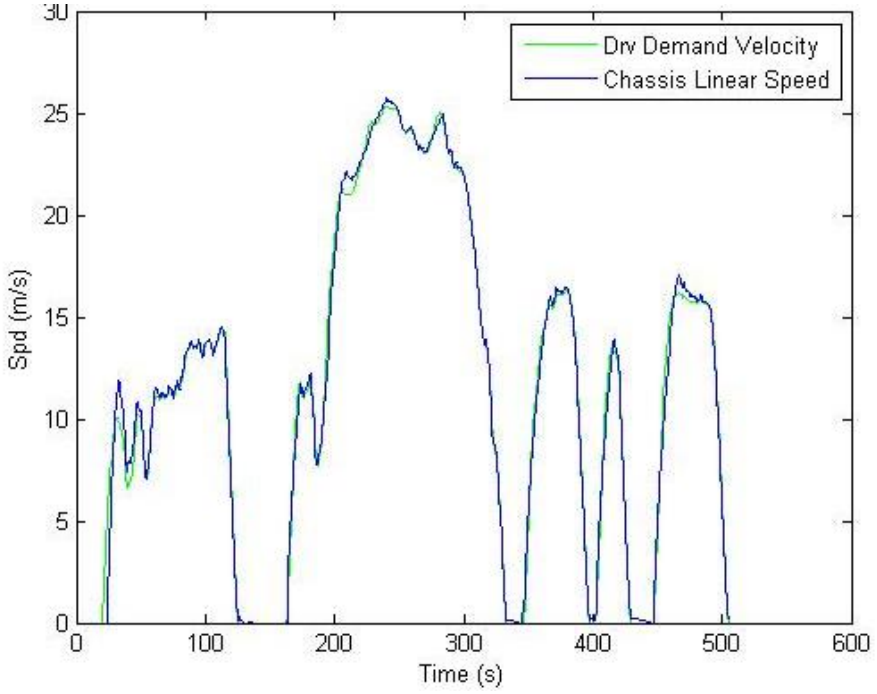

Figure 41: 505 Cycle velocity of the trace

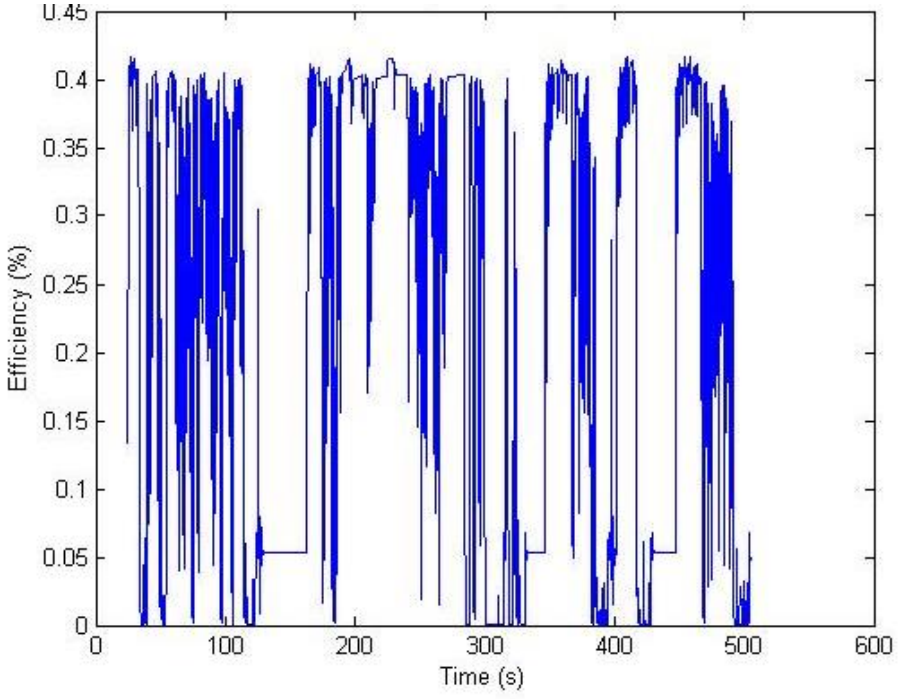

Figure 42: Engine Efficiency 505 cycle with original control strategy

4.5.4.2 Post-Optimization Charge Sustaining Control

The control strategy for charge sustaining with this architecture has two primary options for improvement over the engine-only operation discussed in the previous section. The engine can provide power directly to the road in a parallel operation, or, the transmission can be used to decouple the engine from the road for a series operation. Allowing the engine to run independent of the road speed means that the engine can run at its absolute maximum energy efficiency. These two operations are outlined in more detail below.

4.5.4.3 Parallel Charge Sustaining Operation

The power flow for a parallel CS mode is seen earlier in Figure 32. During this parallel operation, the engine is mechanically connected to the road and, as a result, the engine speed is dictated by a limited number of possible gear ratios and the linear speed of the vehicle. This mechanical connection causes the engine to operate at an angular velocity that produces sub-optimal efficiency. Despite this limitation, the electrification of the powertrain does allow the engine to operate at a higher efficiency through an ability to control torque.

As can be seen in Figure 26, the engine can have a high efficiency at many angular velocities so long as an optimal torque is requested. Lower torque demands that operate at the worst efficiencies can be avoided by using the electrified powertrain as a generator, thus increasing the engine torque demand. Conversely, when requesting an engine torque that is higher than its optimal torque, the efficiency can be improved by reducing the demand torque on the engine by injecting torque from the electric motors to reach an ideal efficiency. It is noted however, that this second situation will not be encountered by UWAFT given that the Weber MPE850t exhibits its highest approximated energy efficiency very near its peak torque. Consequently, the potential benefits of using electrified components to reduce the torque demand upon the engine is not examined in this paper.

The analysis for this operation is done in terms of wheel torque demand and linear speed, similar to the previous EV mode analysis. It is noted that the P2 is the only motor used for generation in this analysis, as the P3 motor in its post transmission position would have increased generation inefficiency through the transmission and torque converter. Thus, the two power flow options examined are the engine running to satisfy the demand and the engine running at an optimal

torque with an electric generation component. Generation occurs using wheel torque and the vehicle's linear speed as inputs and its efficiency is compared for each gear.

The first option's efficiency is a combination of the engine's performance at demand torque, the torque converter efficiency and the transmission efficiency. Note that the engine-only mode simulates the engine without electrification assistance.

The second option has an increased model complexity as it is a dynamic system where not all the power goes through the same powertrain devices over the entire vehicle drive cycles. This option's overall energy efficiency is then calculated with a multi-step approach. First, the energy efficiency of the engine at an optimal torque is utilized. Next, the power that is requested is put through the torque converter and the transmission. Finally, the remaining portion of optimally generated power which is over the demanded output is put through the P2 generator energy efficiency map and battery energy efficiency map to develop an average efficiency which is then used to estimate the EV output. Given that the future torque/speed request is unknown at the time of power generation, it is assumed that when CS halts and EV is transitioned to, that the average output efficiency is 90%. For this report, an average value of 90% is used for future EV output energy efficiency.

Once these two efficiency maps are created for all six gears, they are compared, and a maximum overall energy efficiency is extracted. For each of the maximum efficiencies, the gear selection and difference between the optimal generation torque and the driver's demanded torque is saved. The resulting peak efficiency, its gear, and the difference in system efficiencies between optimal torque and the demanded torque are seen in Figure 43, Figure 44, and Figure 45 respectively. It can be seen that the difference is always negative, meaning that the optimal engine operation is always more or equally as efficient for this model.

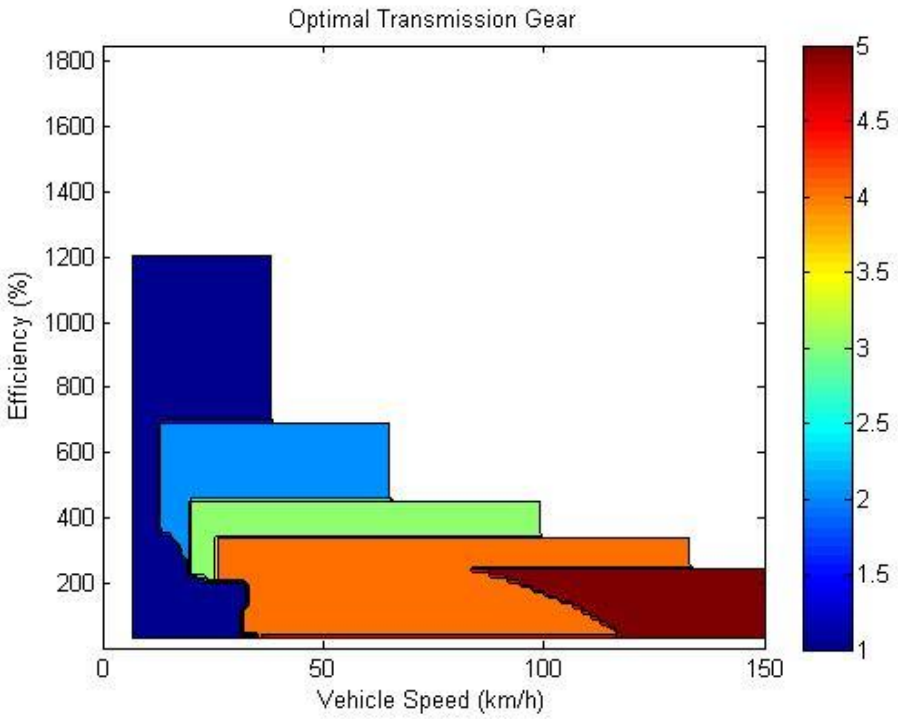

Figure 43: Gear for maximum efficiency

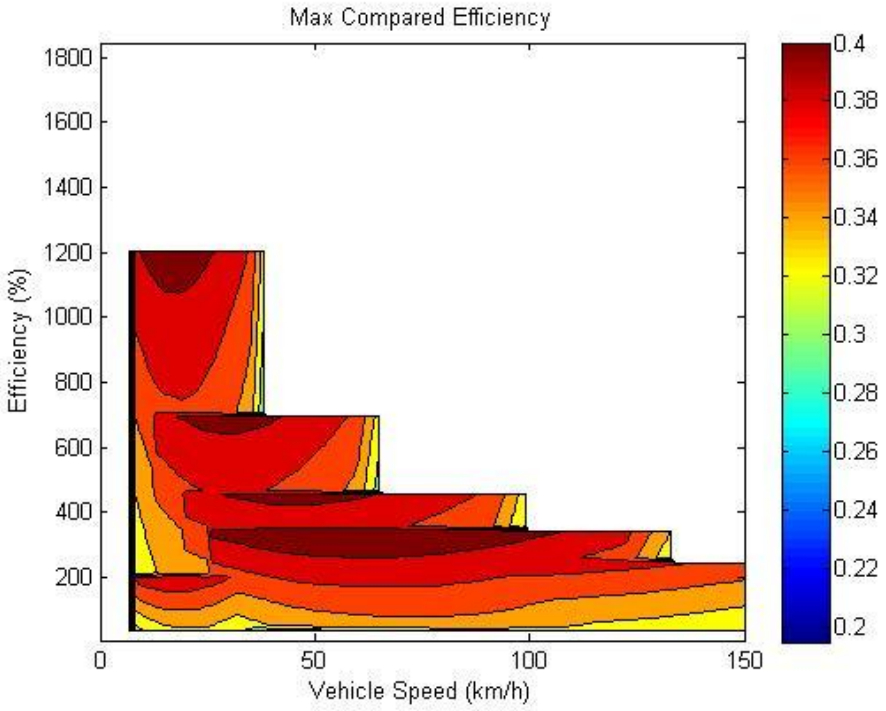

Figure 44: Maximum system efficiency parallel

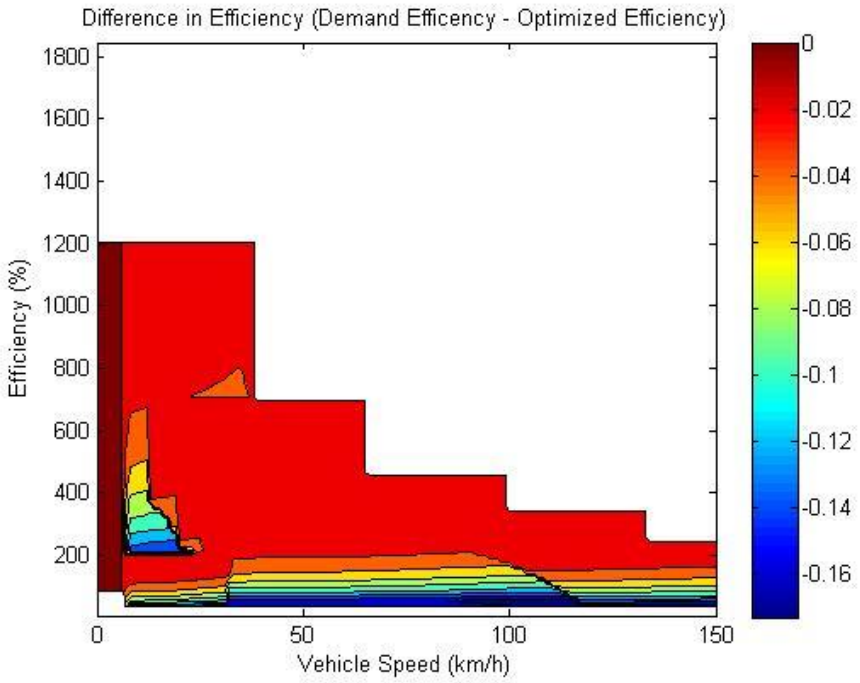

Figure 45: Efficiency difference between optimal operation and demand torque operation

4.5.4.4 Series Charge Sustaining Operation

The power flow for Series CS mode can be seen in Figure 33. In this drive mode the transmission is put into neutral, which decouples the pre-transmission components mechanically from the road. With this configuration, the engine and generator (P2 motor) are now able to operate at a speed independent of road speed with a 1:1 ratio coupling between them. Within this series operation, there are two significant control operations to investigate.

The first control operating mode is thermostatic, during which the engine and generator operate at the angular speed and torque which provides a maximal generation efficiency. This operation results in constant power generation, independent of the power requested by the driver. For the developed model, this generation mode results in a peak energy efficiency of 39.3%, a value which is the combined generator and engine efficiency. This value is calculated with the energy efficiency map seen in Figure 46. Note that the energy developed is stored in the battery and can

then be used by the P3 motor to propel the vehicle. In addition, due to the powertrain path being decoupled from the engine speed from the road, this system bypasses the efficiency loss of the torque converter and transmission. There are other efficiency losses however, as during series operation the power goes through the generator (the P2 Motor) and then through the electrified drive train again into the P3 motor. This transition from mechanical energy to electric energy and back into mechanical energy represents a significant efficiency loss; a minimum of 90% given the peak efficiencies of the motors and battery onboard the vehicle. Additionally, while running in series only the P3 motor is available for propulsion which, as has been explored in the previous EV operation section, is not as efficient as a two-motor strategy. The P3 motor is only able to perform efficiently when the vehicle is moving at high speeds, causing the vehicle to only operate in thermostatic operation when sustaining highway speeds.

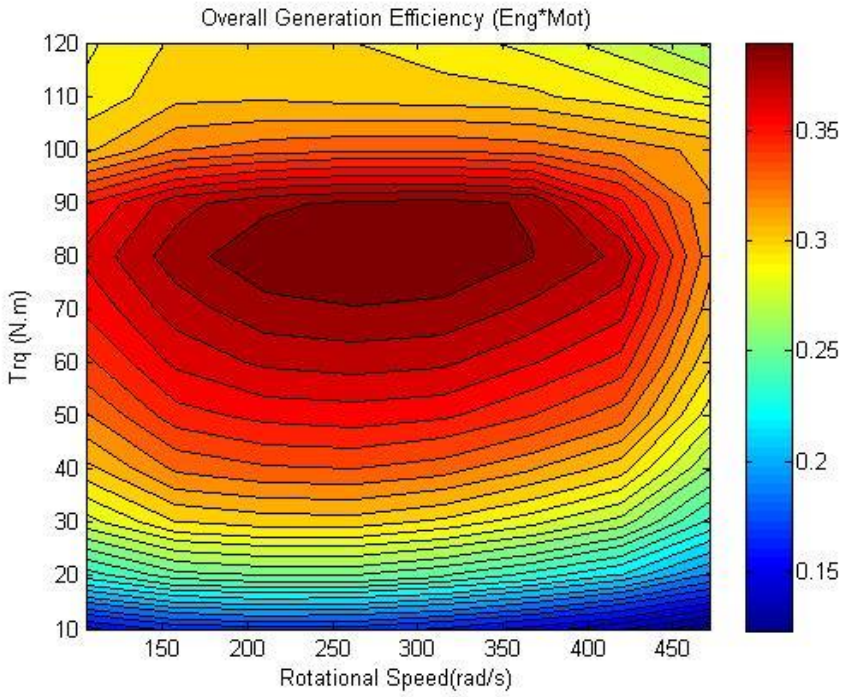

Figure 46: Series Generation Efficiency Map

The second possible CS mode series operation is a load following operation. During this operation mode, the engine and generator combination will generate the power requested from the driver at the most efficient speed and torque for that power. The power generation does not have to precisely follow the load generation, as the battery will supplement power or absorb extra generated power, acting as a buffer. To implement load following, the peak energy

efficiency for each power output is required. Using the generation efficiency map with power increments of 3 [kW], the peak energy efficiency is determined and shown in Figure 47. Note that peak efficiencies are determined as the maximal energy efficiency for each 3 [kW] set of efficiencies. Each of the points on this map have an associated speed and torque for the engine-generator coupling. Using this relationship, a lookup table is then implemented to determine the energy efficiency, speed and torque for load following generation. Due to the significant decrease in efficiency and the need for the mechanical-electrical-mechanical energy transition, the series load following is not employed while running the vehicle.

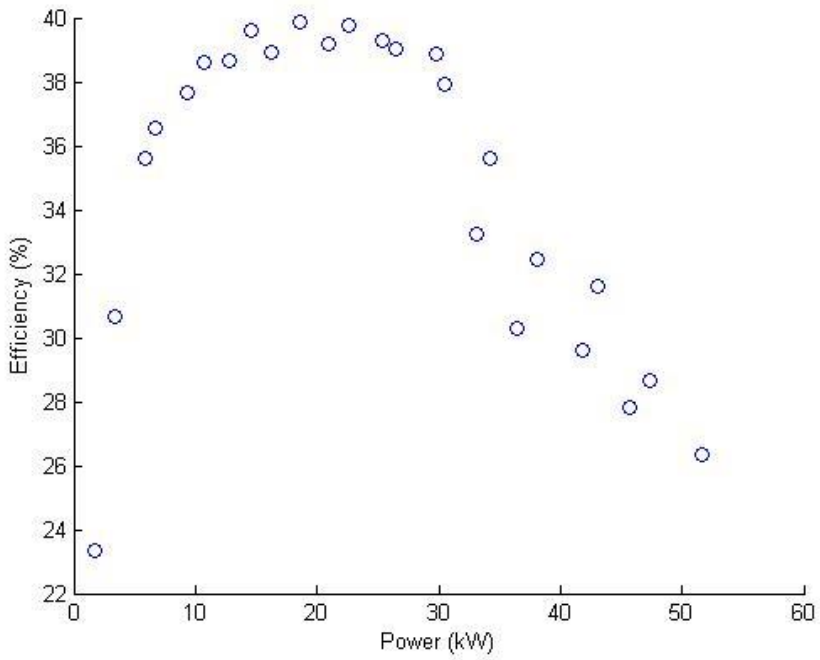

Figure 47: Efficiency vs Power for load following

4.6 Results

The engine efficiency when using the optimized strategy is shown in Figure 48. The plateaus that are visible seen in this map are a result of employing the optimized generation strategy. When the vehicle torque request is below the optimal torque at the engine, the motors then request generation at the optimal point and this also creates a plateau. The extended plateau at the highest energy efficiency at just after 200 seconds is when the vehicle enters a thermostatic

series operation, and the system is able to operate at maximum energy efficiency independent of vehicle speed.

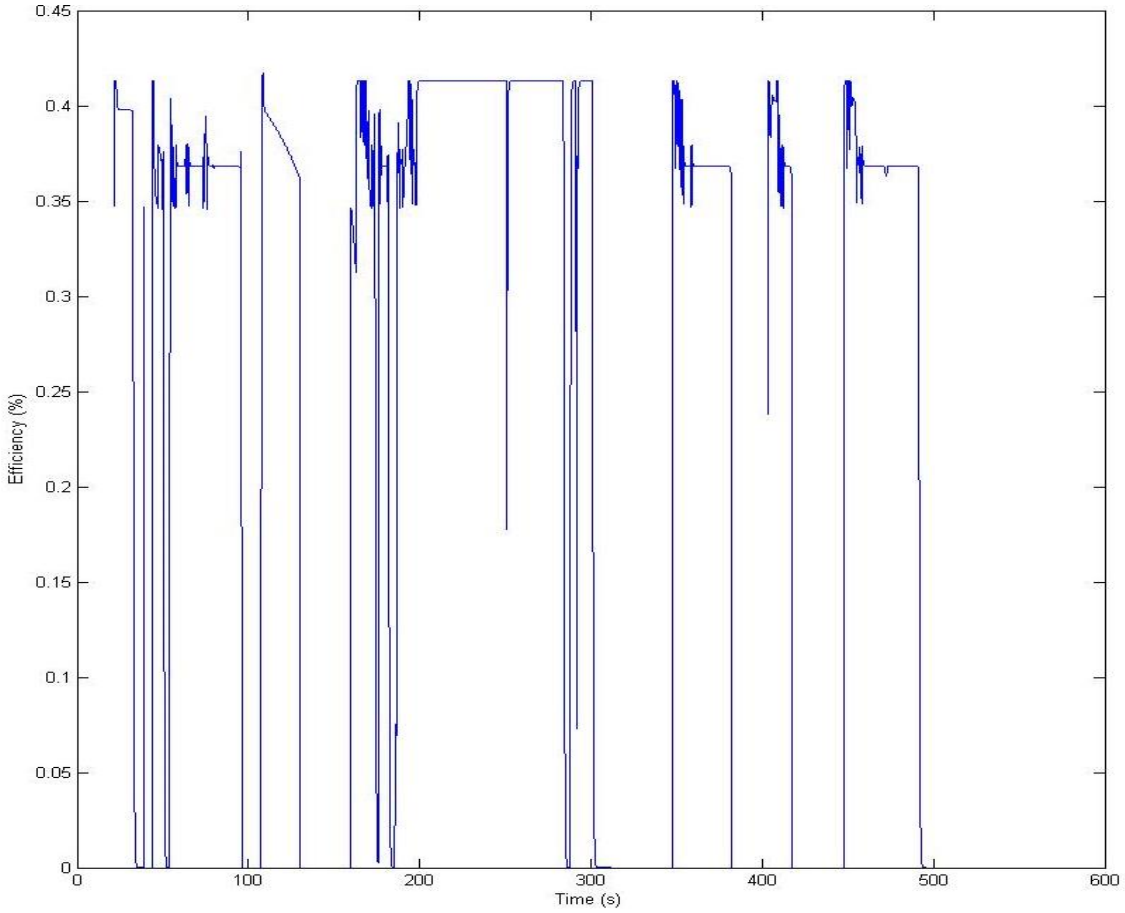

Figure 48: Engine Efficiency during optimal control operation

Modeling Results**Error! Reference source not found.**shows the results for the model based on standard set of cycles: the US06 City, the US06 Highway, the 505, and the HWFET cycle. The results are weighted based on the weighting factors of the EcoCAR 3 competition, seen in Table 11. For CD cycles the vehicle is tested at 90% SOC, while for CS cycles the vehicle is started at 20%. During simulations, UWAFT permitted a maximum SOC change of 1% during CS operation. The total range is calculated with 16 kg of 85% ethanol fuel; this tank size is developed by UWAFT for EcoCAR 3. Note that energy consumption, petroleum use, greenhouse gas emissions, and criteria of emissions are all calculated based upon the EcoCAR 3 Non-Year-Specific Rules (NYSR). Any deviation from the NYSR in UWAFT's calculations is outlined after the results[35].

Table 11: EcoCAR 3 Cycle Weighting Factors

Cycle	US06 City	US06 Highway	505	HWFET
Weighting Factor	14%	45%	29%	12%

It is observed that the optimized control strategies have provided for significant changes to the metrics as outlined in Table 12. In this table, the first column contains UWAFT's Vehicle Technical Targets (VTT). These targets are developed from both modeling results and a market analysis. Additionally, it is noted that the second and third columns of this table represent the model utilizing the basic and optimized control strategies respectively.

In observing simulation results for optimized models, the CD control strategy decreased the energy consumption during CD mode by 13.8% (from 223.44 Wh/km to 192.67), and increased the CD range by 27.7% (from 53.79 km to 68.70). It is noted however that CD fuel consumption did increase during more aggressive drive cycles (from 6.15 Wh/km to 17.6 Wh/km). This increase in consumption is due in part transmission gear switching, which results in a torque provided to the wheel that is less than the demanded torque until the gear change is completed. With implementing the optimized control strategy, this delay comes into effect, and it leads to a prolonged above-threshold accelerator signal. The vehicle then enters performance mode, due to the accelerator signal, which uses the engine to supplement power, thus consuming fuel. It is noted that overall, fuel consumption while meeting torque demands is still greatly reduced from a purely engine-driven operation. Additionally the need to enter performance mode and engage the engine can be removed with a more complicated control strategy using the P3 motor to provide more power during transmission lag.

Optimizing the CS control strategy most significantly increased the miles per gasoline equivalent, creating a 30.5% improvement (from 42.89 mppge to 61.80 mppge). Unfortunately the magnitude of this improvement is suspect to UWAFT. The engine model is the most significant component model in the CS model, and it is a low fidelity model. The peak energy efficiency in this model is based upon that of an ideal E85 engine with a higher compression ratio than typically realized. This modelling fidelity issue significantly reduces the applicability of the CS results.

The total range of the vehicle is however increased by 30.2% (from 303.79 km to 395.67 km). This is a combination of the increased CD and CS energy efficiency. Throughout this testing, the fuel tank has remained constant at 16 kg, but there is a significantly increased use of that fuel during CD operation for the optimized control strategy. The CS range is calculated as a sum of the remaining fuel range and the battery's CD range. Since the developed range satisfies the competition requirements, the tank size can be re-examined for additional weight savings via reduction of size. This is an area of further optimization the team wishes to explore.

Table 12: Modeling results for E&EC Cycle

Specification	UWAFT's VTT	Simulation result	Changed Results
Acceleration, IVM-60mph [s]	5.82	5.6	5.6
Acceleration, 50-70mph (Passing) [s]	6.6	3.2	3.2
Braking, 60-0mph [ft.]	121.4	121	121
Acceleration Events Torque Split (Fr/Rr)	0/100	0/100	0/100
Lateral Acceleration, 300ft. Skid Pad [G]	0.84	N/A	N/A
Double Lane Change [mph]	54.4	N/A	N/A
Highway Grade ability, @60 mph for 20 mins	6%	7%	7%
Cargo Capacity [ft^3]	2.4	2.4	2.4
Passenger Capacity	4	4	4
Vehicle Mass [kg]			
Curb Mass [kg greater than stock]	275	160	160
Starting Time [s]	5	N/A	N/A
Total Vehicle Range [km]	301	303.79	395.67
CD Mode Range [km]	36	53.79	68.70
CD Mode Total Energy Consumption [Wh/km]	267.8	223.44	192.67
CS Mode Fuel Consumption [mpgge]	30	42.89	61.80
UF-Weighted Fuel Energy Consumption [Wh/km]	736.6	232.71	182.7
UF-Weighted AC Electric Energy Consumption [Wh/km]	23.8	116.87	105.4
UF-Weighted Total Energy Consumption [Wh/km]	758	349.59	287.1
UF-Weighted WTW Petroleum Energy Use [Wh PE/km]	621	67.92	53.54
UF-Weighted WTW Greenhouse Gas Emissions [g GHG/km]	222.6	113.93	96.12

UF-Weighted Criteria Emissions [g/km]	2.64	0.402	0.398
Number of Burritos Fit in Glove box [#]	11.5	11.5	11.75

4.6.1.1 Energy Consumption

The SOC-Corrected Fuel Consumption is calculated through the following equations in-place of Equation 18 from the NYSR [35]:

$$FC_{Weighted}\left[\frac{kg}{km}\right] = \frac{FC\left[\frac{L}{100km}\right]}{100} * 0.7871[\frac{kg}{L}]$$

(2)

$$FC_{SOC-c}\left[\frac{kg}{km}\right] = FC_{Weighted}\left[\frac{kg}{km}\right] + \frac{0.000621 * EC\left[\frac{Wh}{mile}\right]}{0.25} / LHV_{fuel}\left[\frac{kWh}{kg}\right]$$

(3)

*EC is electric charge sustaining consumption

*$FC_{soc\text{-}c}$ is the SOC corrected fuel consumption

*$FC_{Weighted}$ is the weighted fuel consumption

Equation (2) converts fuel consumption from [L/100km] to [kg/km] using the density of E85 fuel, 0.7871 [kg/L]. The 0.000621 coefficient in Equation (3) is to convert Wh/mile to kWh/km. The difference between Equation (3) and Equation 18 in the NYSR is that division by drive cycle distance is omitted in Equation (3). This decision is made because Autonomie outputs electrical consumption in Wh/mile instead of kWh, and fuel consumption in [kg/km] is already obtained through Equation (3).

4.7 Technical Merit

The model used in this paper is missing some information which would improve its accuracy. At this stage in the competition the component suppliers have not provided the energy efficiency

maps for all the components. **Error! Reference source not found.**shows some energy onsumption values that, when compared to industry vehicles, might seem implausibly low. Two significant contributors to this discrepancy in the model at the moment is the inverter, and the engine. The efficiency of the inverter is built into the motor energy efficiency map at the moment, but it is likely that the inverter will present more significant efficiency losses than currently modelled. The engine, as described before, is scaled to a peak efficiency of 41%. While this is a possible energy efficiency, it is idealized and only achievable with the high combustion ratios possible with ethanol. Important to note about the results is the swing in energy efficiency more than the magnitude of the energy consumption.

4.8 Conclusion and Recommendations

The vehicle designed by the University of Waterloo Alternative Fuels Team is configured in a split-parallel architecture. This architecture enables the vehicle to operate in different power flow operations and this enables the team to meet performance and energy efficiency targets.

This paper examines optimizing the control strategy of the vehicle's powertrain components in order to maximize energy efficiency across the charge depleting and charge sustaining modes. To model the vehicle, the team used Autonomie, a software wrapper for MATLAB and Simulink which contains a number of component models that the team used to approximate their vehicle. The vehicle model is then modified in Simulink, with a focus upon the main power components including the motor, engine, battery, and transmission.

The basic control strategy for a full electric operation uses only the P3 motor for propulsive power. This mode is used to minimize the amount of the energy that is needed to be transferred through the transmission with its associated inefficiencies. The optimized strategy compared the energy efficiency of both motors and the transmission, finding a maximum energy efficiency that could then be achieved. From this maximum energy efficiency, the transmission gear and motor torque split are developed into a lookup table in the controls of the vehicle. The change in control strategy increased the CD range by 27.7 %. Unfortunately, the CD range is blended and due to the introduction of transmission shift lag into the model, the performance mode gets triggered more during the aggressive drive cycles. This blending operation increases the amount of fuel used in CD operation. Despite this, the CD energy consumption is still decreased by 13.8 %.

In charge sustaining mode, the basic control strategy runs the engine as an internal combustion engine but still regenerates energy during braking. Additionally, the motors would assist if a large acceleration is needed. The logic behind this strategy is that there is minimal to no mechanical-electrical-mechanical power conversion. The optimal control strategy compared the engine efficiency at demand torque, that is, the energy efficiency if running in the basic control strategy, to the energy efficiency of the propulsion system if the motor is used to bring the engine output to an optimal torque. From this comparison, the maximum energy efficiency of system operation was obtained along with the transmission gear, negative motor torque (generation torque) and engine torque to achieve it. The optimized control strategy produced a 30.5% increase in miles per gallon gasoline equivalent, increasing total range by 30.2%. While this improvement shows the potential for an optimized strategy to increase the charge sustaining mode energy efficiency, the magnitude is potentially inaccurate. This error is partially due to the development of an engine efficiency that is coarsely approximated from a high pressure ethanol combustion efficiency and with a small engine efficiency map. It is noted that this map is scaled to the correct torque and power range for the selected MPE850t engine. Additional simulations will be required once a more accurate engine model is developed.

Chapter 5

Just-In-Time Control

The following section is based on previously published work Ellsworth, P., Scott, W., Fowler, M., Fraser, R. et al., "Internal Resistance Optimization Utilizing “Just in Time” Control," SAE Technical Paper 2015-01-1234, 2015, doi:10.4271/2015-01-1234. byEllsworth et.al. [36]This thesis author specific contribution to this paper was to: develop the model, conduct the simulations, prepare all the graphics and results, prepare the final manuscript and reviewer edits with direction and assistance from the project supervisors and research colleague who were co-authors.

5.1 RInt Model

To estimate the benefits of IRB control, the battery resistance as a function of SOC must be determined. The Department of Energy (DOE) has developed a simple equivalent circuit model (ECM) for electrified vehicles which estimates the internal resistance (R_{int}) of Li-ion batteries (Figure 49) [37]. This model is commonly known as the ‘Rint’ model. Using a combination of two diodes and resistors, this model estimates the deviation from the open circuit voltage as a function of SOC and current direction (Eqn. 1). By referencing the internal resistance with respect to SOC, IRB control can be used to minimize the energy loss of modern vehicles.

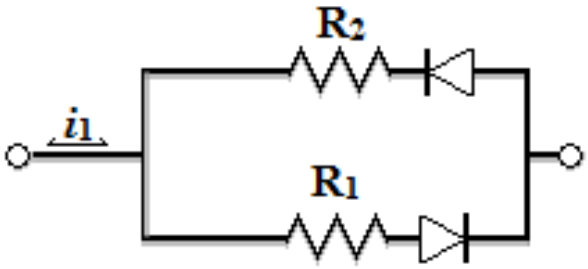

Figure 49: Equivalent circuit model (Rint)

$$V_{model} = V_{oc} - V_{circuit} = V_{OC} - i_1 R_{1|2} \qquad (1)$$

5.2 Test Bench Equipment & Configuration

The test bench schematic and test bench used to perform the HPPC tests are shown in Figure 50 and Figure 51 respectively. The pictured battery cycler is the Maccor 4200^{TM}, which has 16 channels and a current control range of 0.1 – 15 A and a voltage control of 0.0 – 5.0 V per channel [38]. Eight channels are combined in parallel to achieve a maximum current of 120 A using a 4-wire parallel connection, where two low gauge wires deliver current and two high gauge wires measure voltage. The accuracy of the eight combined channels for each battery is ±0.1 A and ±1.0 mV. The current-voltage data is logged each second and every change in 1 mV.

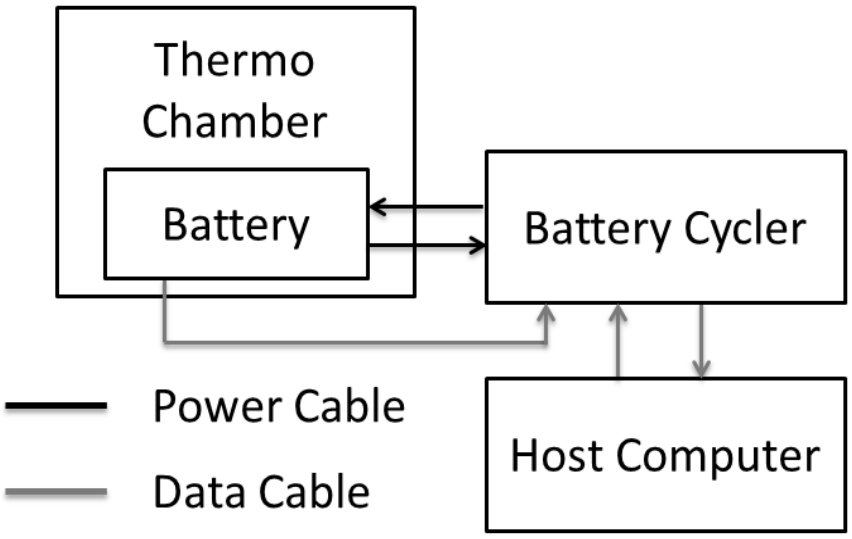

Figure 50: Test bench schematic

The pictured thermo chamber is the SubZeroMicroClimate® 1.2 (Figure 51), which maintained the temperature within ±0.5 K of the set point (23.75 °C) [39]. While inside the thermo chamber, the battery is enclosed in a vice that simulates a pack enclosure (two 4 mm thick inner aluminum plates, which simulate pack fins that distribute heat across the battery surface, inserted between two 5 mm thick acrylic plates, which simulate battery casing).

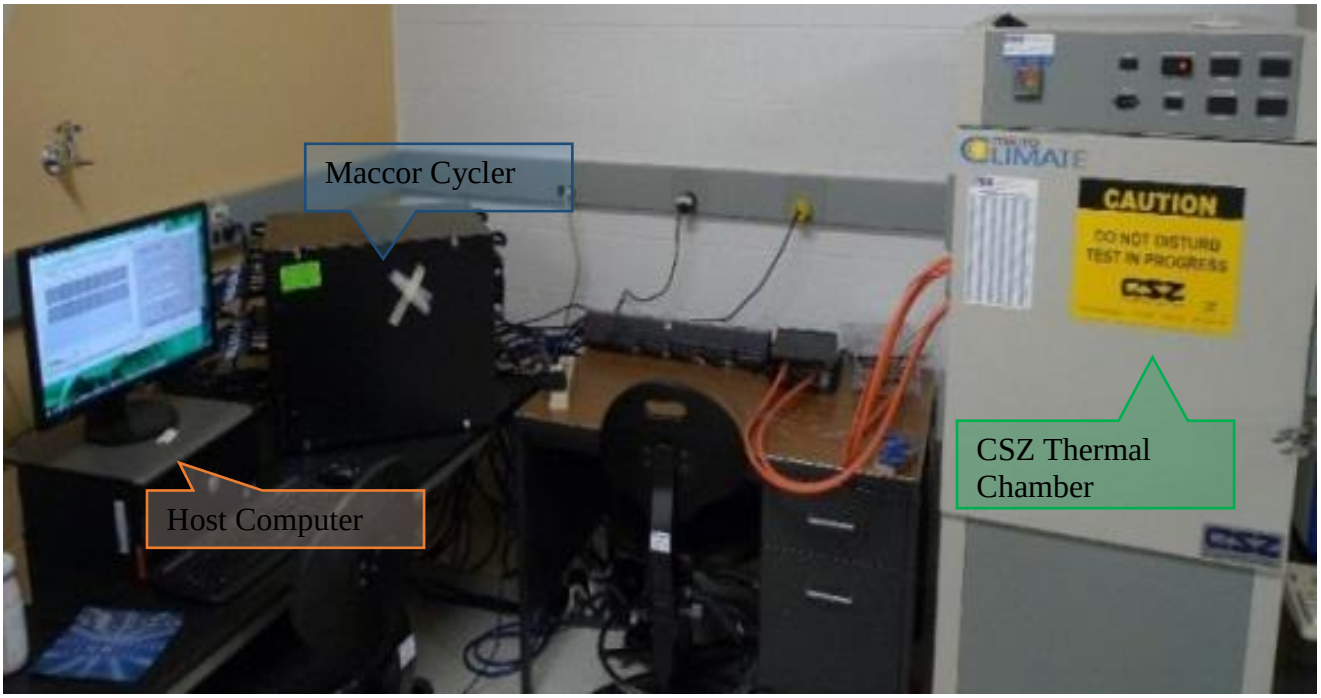

Figure 51: HPPC test bench

The pictured host computer (Figure 51) communicates with the battery cycler via LabView software [40]. All interactions between the test battery and battery cycler are orchestrated through this interface. The thermo chamber is not controlled by the host computer, and is externally monitored. Details of the test battery, designed for EREVs, are given in Table 13.

Table 13: Battery specifications

Parameter	Entry
Cathode Material	$LiFePO_4$ (LFP)
Anode Material	Graphite
Electrolyte	Liquid organic
Capacity range	18-21
Nominal Voltage	3.3
Dimensions (mm)	7.25×160×227
Weight (g)	496

5.3 Modified HPPC Test Procedure

The HPPC test current profile is modified to represent the drive cycle current seen within Autonomie vehicle modeling software, for a UDDS drive schedule (Figure 52). To clarify, the discharge and charge currents are changed from 1 and ¾C to 5 and 3 ¾C respectively.

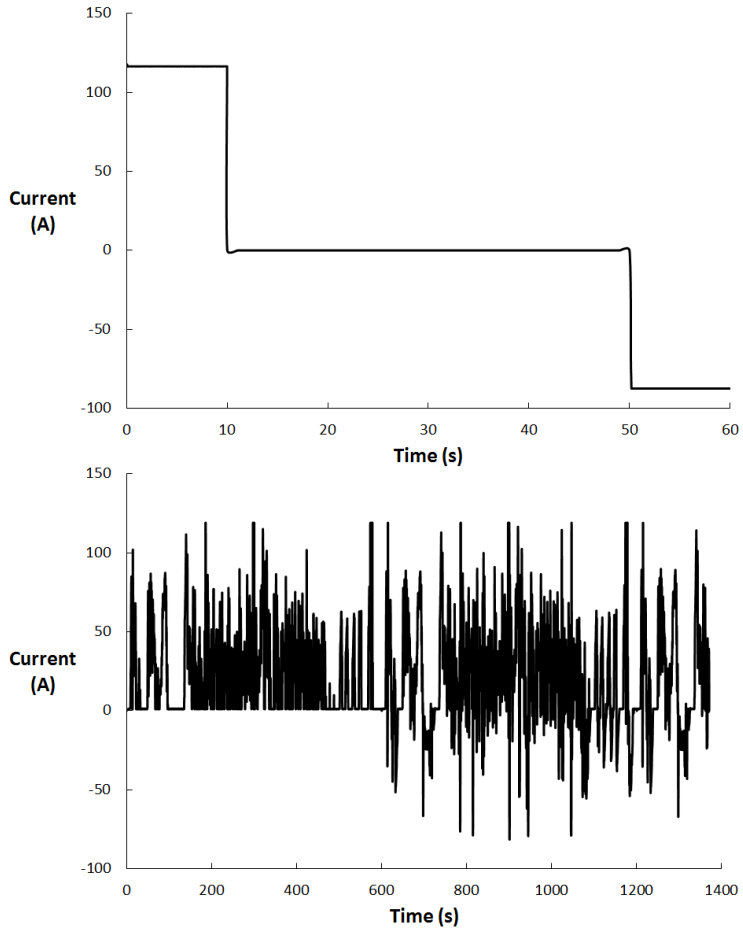

Figure 52: Modified HPPC test (top) and Autonomie generated UDDS drive schedule (bottom) current profiles

The battery is initially characterized by a full charge/discharge cycle. The battery is charged at 1C constant current, followed by a constant voltage charge until the current decreases to C/20. The battery is then rested until equilibrium is reached, defined as a change in voltage smaller than 5 mV over a ½ hour period or a rest period exceeding two hours. The battery is then discharged at 1C constant current until the cut-off voltage is reached, then at constant voltage until the current reaches C/20. The battery is then rested until equilibrium.

The modified HPPC current profile (10 s discharge pulse at 5C, followed by a 40 s rest period, and then a 10 s 3.75C charge pulse) is performed at 5 % SOC intervals, where the voltage response is recorded by the host computer. To reach the desired SOC between tests, the battery is discharged to the cutoff voltage (i.e. manufacturer defined 0% SOC) by the above method, and then charged to the desired SOC by coulomb counting at constant current (1.25C).

5.4 Rint Model Characterization

The HPPC measured voltage response, in conjunction with the Department of Energy (DOE) Partnership for the Next Generation of Vehicles (PNGV) Test Manual [41], is used to characterize the battery internal resistance. For reference, the equations are presented (Eqn. 4 and 5), where V_{t0}&I_{t0},V_{t1}&I_{t1}, V_{t2}&I_{t2}, and V_{t3}&I_{t3} are the voltages and currents measured at 0, 10, 50, and 60 seconds, respectively.The battery charge and discharge resistances, as well as the open circuit voltage, can be viewed in Figure 53. Non-characterized values (i.e. between 5% SOC intervals) are linearly interpolated. Detailed results can be viewed in Table 14 and Table 15 (Appendix A).

$$\boldsymbol{R_{Dis}} = \frac{\Delta V_{discharge}}{\Delta I_{discharge}} = \frac{V_{t1}-V_{t0}}{I_{t1}-I_{t0}} \qquad (4)$$

$$\boldsymbol{R_{Chg}} = \frac{\Delta V_{charge}}{\Delta I_{charge}} = \frac{V_{t3}-V_{t2}}{I_{t3}-I_{t2}} \qquad \textbf{(5)}$$

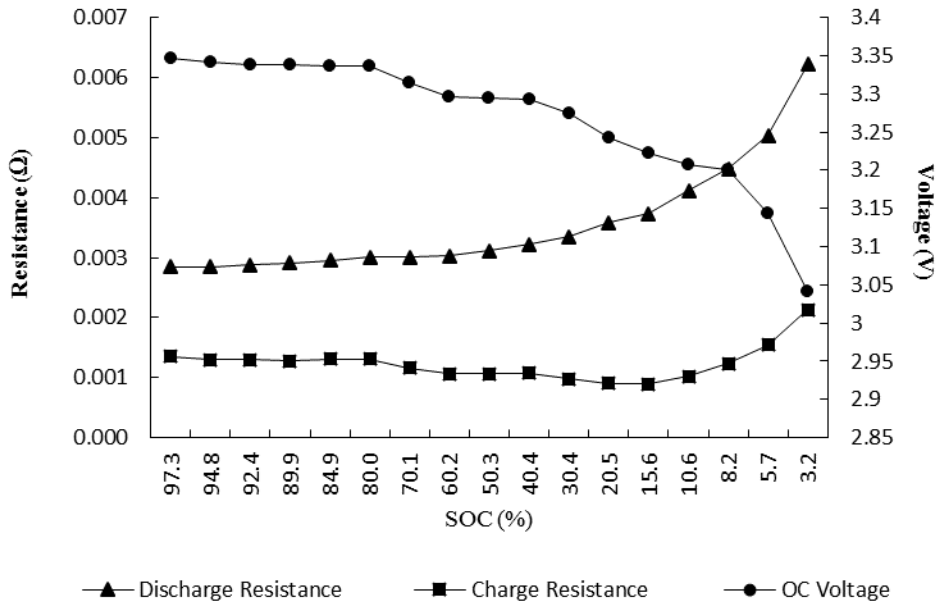

Figure 53: Resistance and open circuit voltage vs. SOC

The ideal SOC operating range is defined as the values that minimize internal resistance (i.e. battery degradation is not considered). When selecting the ideal SOC range, it is assumed that

the discharge and charge resistances are of equal weight (i.e. the lowest sum of discharge/charge resistances is used). In this work, the ideal SOC range is calculated to be 60 %.

While CS mode equates the sum of discharge and charge currents, power loss is a second order function of current. Therefore, as discharge currents tend to be of larger magnitude (Figure 52), the ideal range leans towards a higher SOC than calculated (Figure 53). However, because the resistance differences between 60 and 70 % SOC is small ($\leq 2 \times 10^{-5}\Omega$), the impact of this observation is assumed to be negligible (Figure 53).

5.5 Vehicle Integration

Vehicle performance is estimated using Autonomie, a plug-and-play powertrain and vehicle architecture development software [42]. To represent a battery pack, the test cell is scaled linearly using a 1p-105s (i.e.1 cell in parallel-105 cells in series) configuration to obtain a voltage, max current, and capacity of 350 V, 200 A, and 6.3 kWh, respectively. The pre-described Rint model is imported into the software interface and used in conjunction with an existing vehicle model to produce the following results.

The Autonomie vehicle used is the "Series Engine HEV MotorWithFixedGear 2wd Midsize" model [42]. All components, other than the ESS, are default Autonomie components validated by Argonne Labs [43]. This vehicle is an extended range electric vehicle (EREV) with characteristics and powertrain depicted inTable 16 and Figure 55 respectively (Appendix B). This EREV is selected for the simple charge depletion (i.e. not blended) strategy, which places emphasis on the control scheme[23]. Note that the proposed control strategy provides similar results for plug-in hybrid electric vehicles (PHEVs), which share a similar control scheme.

Two simulations are performed using the urban domestic drive schedule (UDDS): the first representing the ideal charge sustain point (60 % SOC), and the second representing the charge sustain point seen in industry (19 % SOC) [21]. The ideal SOC range is shown to conserve approximately 15 Wh of energy throughout the drive schedule (Figure 54). In other terms, the net energy loss over the drive cycle is 14 % less than those seen in industry modeled results for the test battery, or the net battery efficiency has been shown to increase from 96.8 to 97.3 %.

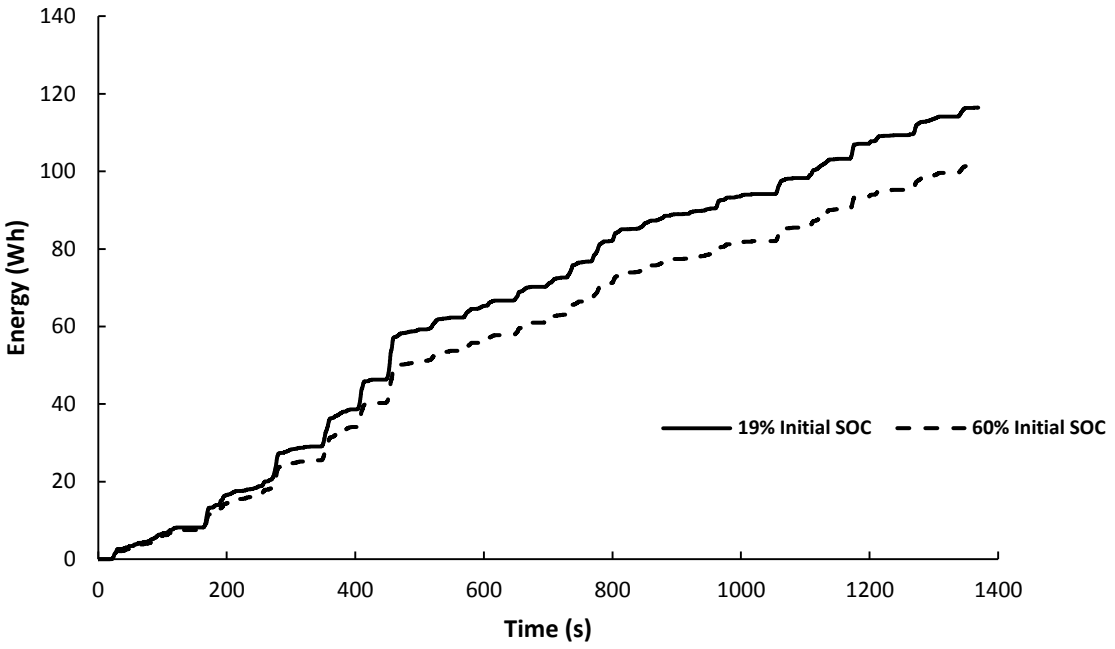

Figure 54: Comparative cumulative energy loss

5.6 Application

The Internal Resistance Based (IRB) control strategy requires that the vehicle is capable of predicting the required energy to reach the final destination. This difficulty is overcome by integration with on board GPS navigation systems. Alternatively, the control system can be implemented with respect to standardized velocity maps used in drive schedules (e.g. UDDS, HWFET, US06) or vehicle competitions (e.g. Advance Vehicle Technology Competitions).

There are indirect benefits to the proposed control strategy other than the direct benefit of increased energy efficiency. The primary indirect benefit is an increased applicable SOC range, allowing the cell to fully discharge (i.e. 0 % SOC) at decreased detriment to the battery similar to an electric vehicle [21][24]. Another indirect benefit is, because charge sustaining mode is activated intermediately (i.e. on the highway, in the middle of the trip) rather than terminally (i.e. in the city, at the end of the trip), carbon emissions may decrease in populated areas. Lastly, lower internal resistance results in decreased heat generation, which has been shown to heavily impact performance [44].

The simulation is composed of individual component models. Simulation fidelity is limited as the component models are isolated from inter-component interference (e.g. vibrations, thermal gradients, and ground loops)

5.7 Conclusion and Recommendations

The presented research shows the benefits of implementing the Internal Resistance Based (IRB) control with minimum internal resistance optimization. Vehicle powertrain modeling yields a net battery efficiency increase from 96.8 to 97.3 % (a 0.5% increase) with an associated 14 % decrease in energy losses across the urban domestic drive schedule. The optimization is performed utilizing the Rint equivalent circuit model at 23.75 °C. If coupled with a known drive distance, obtained from GPS integration or predefined velocity maps, benefits include higher battery efficiency, an increased active SOC range, decreased urban emissions, and decreased waste heat generation.

Chapter 6
Conclusions and Recommendations

6.1 Conclusions

A number of advanced hybrid vehicle technologies and strategies have been examined in this work. The tests and experiments ranged from component development to vehicle control. These experiments outline a number of ways to increase the efficiency of a vehicle, decrease emissions; while maintaining customer appeal and performance through an electrified powertrain. The first phase explored converting a small gasoline engine to ethanol and then its operation within the performance hybrid architecture.

- The dynamometer setup and aftermarket engine controller are able to effectively run the engine
- 58 % of specified torque and 65 % torque can be achieved for a steady state operation using ethanol
- Speed matching capabilities were tested and implemented in a new model
- Updated model illustrated how the engine will allow the vehicle to meet highway speed charges sustaining requirements
- Comparing series and parallel operation shows that at highway speeds parallel operation is more efficient

In the second phase the scope was that of the vehicle level control architecture.

- Leveraging the unique aspects of the vehicle powertrain the CD range by 27.7 % and decreased energy consumption by 13.8 %
- Optimized CS operation produced a 30.5 % increase in miles per gallon
- The total range was increased by 30.2 %
- Optimizing the power flow within the vehicle can significantly increase the energy efficiency and range of the vehicle despite increasing complexity

The final phase explores the future of vehicle level control, using Just-in-Time Control.

- Just-in-Time optimized strategy yields a battery efficiency increase from 96.8 to 97.3 %

- Leading to a 14 % decrease in energy lost within the battery during a UDDS drive cycle

6.2 Recommendations

As mentioned in Subsection 6.1 this thesis demonstrated a number of efficiency improvements. The following recommendations will allow further understanding of the efficiency impacts. In the engine tuning component:

- Continue to improve the tune on the engine and generate new maps performance data
- Further analysis is required for low speed operation

The next steps for the operating mode optimization phase is to:

- Update component models with validated data
- Validate with vehicle level drive cycles

To further research in the internal resistance optimization phase:

- expand the model testing to more
    - Drive cycles
    - Battery temperatures
- Validation testing using an actual vehicle or pack

References

[1] Wikipedia, "Hybrid Electric Vehicle Sales in the United States," [Online]. Available: https://en.wikipedia.org/wiki/Hybrid_electric_vehicles_in_the_United_States. [Accessed 7 April 2016].

[2] S. C. Davis, Transportation Energy Data Book: Edition 33, ORNL-6990, Oak Ridge: Oak Ridge National Laboratory, 2014.

[3] National Highway Traffic Safety Administration, "CAFE - Fuel Economy," 2015. [Online]. Available: http://www.nhtsa.gov/fuel-economy/. [Accessed 27 April 2015].

[4] E. Tate, M. Harpster and P. J. Savagian, "The Electrification of the Automobile: From Conventional Hybrid, to Plug-in Hybrids, to Extended-Range Electric Vehicles," *SAE International,* vol. 1, no. 1, pp. 2008-01-0458, 2008.

[5] A. G. Boulanger, C. A. Chu, S. Maxx and D. L. Waltz, "Vehicle Electrification: Status and Issues," *Proceedings of the IEEE,* vol. 39, no. 6, pp. 1116-1138, 2011.

[6] M. Ehsani, Y. Gao and A. Emadi, Modern Electric, hybrid Electric, and Fuel Cell Vehicles: Fundamentals, Theory, and Design, Second Edition, Boca Raton: CRC Press, 2009.

[7] S. C. Davis, S. W. Diegel and R. G. Boundy, "Transportation Energy Data Book - Edition 33," Oak Ridge National Laboratory, Oak Ridge, 2014.

[8] Argonne National Laboratories, "Sponsors," [Online]. Available: http://ecocar3.org/wp-content/uploads/2015/01/Sponsor-Brochure_1-28-15.pdf. [Accessed 2nd April 2016].

[9] J. Neubauer, A. Brooker and E. Wood, "Sensitivity of plug-in hybrid electric vehicle economics to drive patterns, electric range, energy management, and charge strategies," *Journal of Power Sciences,* vol. 236, pp. 357-364, 2013.

[10] A. Seaman, T.-S. Dao and J. McPhee, "A survey of mathematics-based equivalent-circuit and electrochemical battery models for hybrid and electric vehicle simulation," *Journal of Power Sources,* vol. 256, pp. 410-423, 2014.

[11] L. A. Graham, S. L. Belisle and C.-L. Baas, "Emissions from light duty gasoline vehicles operating on low blend ethanol gasoline and E85," *ScienceDirect,* vol. 36, no. 3, pp. 1233-1235, 2008.

[12] Rodríguez-Fernández, T. Theinnoi, Snowball and Sawtell, "BioEthanol for Sustainable

Transport - BEST Project," *SAE,* pp. 2,3, 2008.

[13] L. Eriksson, T. Lindell and O. L. a. A. Thomasson, "Scalable Component-Based Modeling for Optimizing Engines with Supercharging, E-Boost and Turbocompound Concepts," *SAE International,* no. 2012-01-0713, p. 1, 2012.

[14] Koch, M. J. Atkins and a. C. Robert, "A Well-to-Wheel Comparison of Several Powertrain Technologies," *SAE International,* no. 2003-01-0081, p. 4, 2003.

[15] Y. K. B, R. Sharma, A. Yadav and M. N. a. T. Sahoo, "Optimal Torque Handling in Hybrid Powertrain," *SAE International,* no. 2013-26-0068, 2013.

[16] B. Gao, Q. Liang, Y. Xiang, L. Guo and H. Chen, "Gear ratio optimization and shift control of 2-speed I-AMT in electric vehicle," *Mechanical Systems and Signal Processing,* vol. 50, no. 51, pp. 615-631, 2015.

[17] G. Wager, M. P. McHenry, J. Whale and T. Braunl, "Testing energy efficiency and driving range of electric vehicles in relation to gear selection," *Renewable Energy,* vol. 62, pp. 303 - 312, 2014.

[18] "High Power Lithium Ion ANR26650," A123, 2006. [Online]. Available: https://altitec.no/media/pdf/ANR26650M1.pdf.

[19] S. Moura, "Tradeoffs between battery energy capacity and stochastic optimal power management in plug-in hybrid electric vehicles," *Journal of Power Sources,* POWER-12509, 2009 .

[20] E. Samadani, "Modeling and Evaluation of Li-Ion Battery Performance Based on the Electric Vehicle Field Tests," *SAE Technical Paper,* doi:10.4271/2014-01-1848.

[21] A. N. Laboratory, "Transportation Technology R&D Center," [Online]. Available: http://www.transportation.anl.gov/D3/. [Accessed 26 10 2014].

[22] K. Kato, "PSOC cycle testing method for lithium-ion secondary batteries," *Journal of Power Sources,* 2002.

[23] J. Gonder and T. Markel, "Energy Management Strategies for Plug-In Hybrid Electric Vehicles," *SAE Technical Paper Series,* vol. 01, no. 0290, 2007.

[24] U.S. Department of Energy, ""Plug-In Hybrid Electric Vehicle R&D Plan"," 2007.

[25] R. DeVault, ""Just-In-Time" Battery Charge Depletion Control for PHEVs and E-REVs for Battery Life," *SAE Technical Paper,* pp. doi:10.4271/2009-01-1384, 2009-01-1384.

[26] Delagrammatikas and M. B. a. G. J., "Advanced Development and Dynamometer Tuning of a Suzuki GSXR 600cc Engine for an FSAE® Vehicle," *SAE International,* no. 2010-01-0310, pp. 6-7, 2010.

[27] GM Autority, "GM 3.6 Liter V6 LFX Engine," 2015. [Online]. Available: http://gmauthority.com/blog/gm/gm-engines/lfx/. [Accessed 3rd April 2016].

[28] Wasteland Performance, "MPE 850 Four Stroke Engine," Wasteland Performance, Minneapolis, 2016.

[29] P. Ellsworth, R. Fraser, M. Fowler, D. VanLanen and B. Gaffney, "Control Analysis for Efficiency Optimization of a High Performance Hybrid Electric Vehicle with Both Pre and Post Transmission Motors," *SAE International,* no. 2016-01-1253, p. 4, 2016.

[30] D. Petitjean, L. Bernardini, C. Middlemass and S. Shahed, "Advanced Gasoline Engine Turbocharging Technology for Fuel Economy Improvements," *SAE Technical Paper,* no. 2004-01-0988, 2004.

[31] S. Shahed and K. Bauer, "Parameteric Studies of the Impact of Turbocharging on Gasoline Engine Downsizing," *SAE International,* no. 2009-01-1472, 2009.

[32] Weber Motor, "MPE 850 Four Stroke Engine," 2015. [Online]. Available: http://www.weber-motor.com/fileadmin/templates/w-motor/content/produkte/specsheets/WM_spec_MPE850Fourstroke_engl.pdf. [Accessed 6 May 2015].

[33] J. Szybist, M. Foster, W. R. Moore, K. Confer, A. Youngquist and R. Wagner, "Investigation of Knock Linited Compression Ratio of Ethanol Gasoline Blends," SAE International, Warrendale, 2010.

[34] Independent Electricity System Operator, "Supply Overview," Independent Electricity System Operator, 23 March 2015. [Online]. Available: http://www.ieso.ca/Pages/Power-Data/Supply.aspx. [Accessed 29 April 2015].

[35] EcoCAR 3, "Non-Year-Specific Rules Revision: C," Chicago, 2014.

[36] P. Ellsworth, "Internal Resistance Optimization Utilizing "Just in Time" Control," *SAE,* no. 2015-01-1234, 2015.

[37] Idaho National Laboratory, "Battery Test Manual," U.S. Department of Energy, 2008.

[38] Maccor Battery & Test Equipment , *4200 Series Startup,* Tulsa: Maccor, 2012.

[39] Cincinnati Sub-Zero, *Installation Operation Maintenance Manual MicroClimate - Series,*

Cincinnati Sub-Zero, 2011.

[40] LabView, "Labview Design Software," National Instruments, 2014. [Online]. Available: ni.com/labview. [Accessed 26 10 2014].

[41] Idaho National Laboratory, "Battery Test Manual For Plug-in Hybrid Vehicles; Rev 0," U.S. Department of Energy, Vehicle Technologies Program, INL/EXT-07-12536, March 2008.

[42] Argonne Nation Laboratory, "Autonomie," U.S. Department of Energy, [Online]. Available: http://www.autonomie.net/overview/index.html. [Accessed 26 10 2014].

[43] Argonne Labs, "Autonomie," Department of Energy, February 2010. [Online]. Available: http://www.autonomie.net/overview/presentations_validation.html.

[44] E. Samadani, "Impact of Temperatire on the A123 Li-Ion Battery Performance and Hybrid Electric Vehicle Range," *SAE Technical Paper*, pp. doi:10.4271/2013-01-1521, 2013-01-1521.

Appendix A – HPPC Test Results

Table 14, and Table 15 below show the data collected on the battery cell used for internal resistance calculations.

Table 14: Cell Details for HPPC Test

Capacity (Ah)			Estimated Values (%)	
Initial	**Final**	**Avg.**	**SOC**	**DOD**
0.486	0.568	0.527	0.9731	0.0268
0.971	1.053	1.012	0.9483	0.0516
1.456	1.538	1.497	0.9235	0.0764
1.942	2.023	1.982	0.8988	0.1011
2.912	2.994	2.953	0.8492	0.1507
3.882	3.964	3.923	0.7997	0.2002
5.823	5.905	5.864	0.7007	0.2992
7.764	7.846	7.805	0.6016	0.3983
9.705	9.786	9.745	0.5026	0.4973
11.646	11.727	11.686	0.4035	0.5964
13.587	13.668	13.627	0.3044	0.6955
15.528	15.609	15.568	0.2054	0.7945
16.498	16.579	16.538	0.1558	0.8441
17.469	17.55	17.509	0.1063	0.8936
17.954	18.034	17.994	0.0816	0.9183
18.439	18.519	18.479	0.0568	0.9431
18.924	19.004	18.964	0.0321	0.9678

Max Capacity = 19.593 Ah

Table 15: HPPC Test Results

SOC (%)	DOD (%)	OCV (V)	R_{Chg} (Ω)	R_{Dis}(Ω)
97.3	2.7	3.347	0.00135	0.00285
94.8	5.2	3.341	0.00129	0.00285
92.4	7.6	3.339	0.00129	0.00288
89.9	10.1	3.338	0.00128	0.00291
84.9	15.1	3.337	0.00130	0.00295

80.0	20.0	3.336	0.00130	0.00301
70.1	29.9	3.314	0.00115	0.00301
60.2	39.8	3.297	0.00106	0.00303
50.3	49.7	3.294	0.00106	0.00312
40.4	59.6	3.293	0.00107	0.00322
30.4	69.6	3.274	0.00097	0.00335
20.5	79.5	3.243	0.00090	0.00358
15.6	84.4	3.222	0.00089	0.00373
10.6	89.4	3.207	0.00102	0.00411
8.2	91.8	3.201	0.00123	0.00447
5.7	94.3	3.144	0.00154	0.00503
3.2	96.8	3.041	0.00213	0.00622

Appendix B – Vehicle Model Inputs & Powertrain

Table 16 and Figure 55 detail the vehicle model that was used to gain full vehicle simulation.

Table 16: Vehicle component powers

Component	Power	Gear Ratio
Engine	70 kW	N/A
Gen	65 kW	N/A
Traction Motor	115 kW	N/A
Final Drive	N/A	4.438

Figure 55: Autonomie Model of the Vehicle